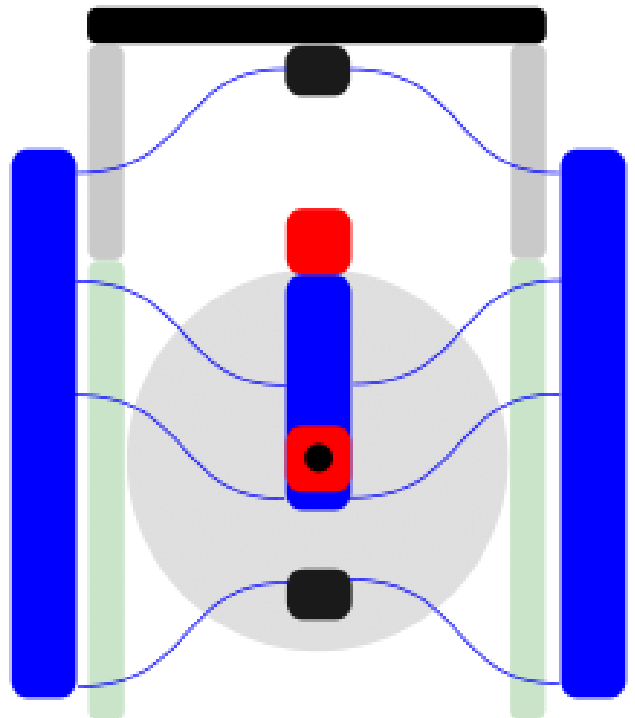
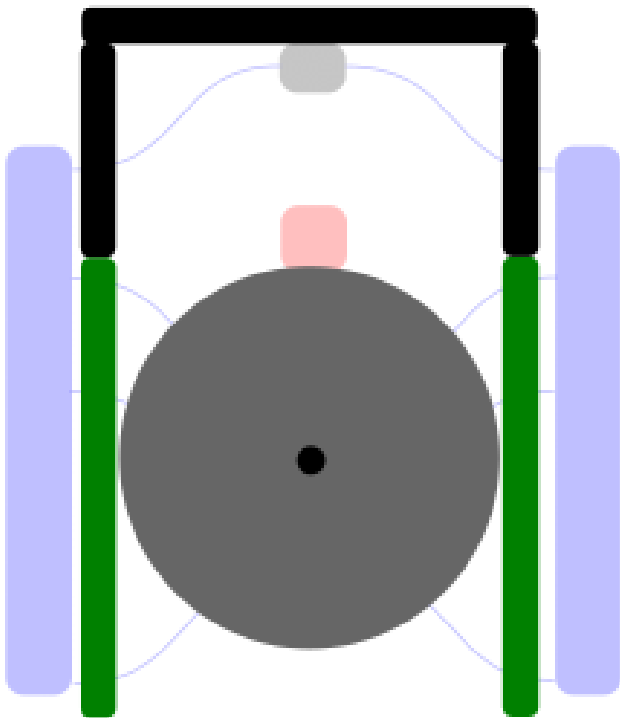


Department of Precision and Microsystems Engineering

A new type of energy harvester for traffic induced bridge vibrations

Michael van den Bergh

Report no : 2023.004  
Coach : Ir. E. van de Wetering  
Professor : Dr.ir. J.F.L. Goosen  
Specialisation : ED  
Type of report : MSc Thesis  
Date : 4 January 2023





# A new type of energy harvester for traffic induced bridge vibrations

by

M.J.N. (Michael) van den Bergh

to obtain the degree of Master of Science

at the Delft University of Technology,

to be defended publicly on Wednesday January 18, 2023 at 09:30 AM.

Student number: 4518586  
Project duration: September 1, 2021 – January 18, 2023  
Thesis committee: Dr. ir. J.F.L. Goosen, TU Delft, supervisor  
Dr. F. Farhadi Macheuposhti, TU Delft  
Dr. A. G. Dunning, Kinergizer  
Ir. E. van de Wetering, Kinergizer

*This thesis is confidential and cannot be made public until January 31, 2023.*

An electronic version of this thesis is available at <http://repository.tudelft.nl/>.



# Contents

<b>1</b>	<b>Introduction</b>	<b>1</b>
1.1	Energy harvesting . . . . .	1
1.2	Energy harvesters in bridge health monitoring . . . . .	2
<b>2</b>	<b>Ambient excitations in bridges</b>	<b>3</b>
2.1	Introduction . . . . .	3
2.2	Measured excitations in the frequency domain . . . . .	3
2.3	Measured excitations in the time domain . . . . .	5
2.4	Conclusion on bridge vibrations . . . . .	9
<b>3</b>	<b>Literature review</b>	<b>11</b>
3.1	Introduction . . . . .	11
3.2	Mechanisms in harvesters . . . . .	12
3.2.1	Power takeoff mechanism . . . . .	12
3.2.2	Transducing mechanism . . . . .	12
3.3	Classification . . . . .	12
3.3.1	Classes . . . . .	12
3.3.2	Non-suspended EH . . . . .	13
3.3.3	Suspended systems . . . . .	17
3.4	Results . . . . .	19
3.5	Discussion . . . . .	23
3.6	Conclusion . . . . .	23
<b>4</b>	<b>Design</b>	<b>25</b>
4.1	Main design direction. . . . .	25
4.2	Design method . . . . .	26
4.3	Effect of main design direction choice on design objective. . . . .	27
4.4	Sub-functions . . . . .	28
4.5	Choosing sub solutions for the design. . . . .	29
4.5.1	Orientation of rotational axis . . . . .	29
4.5.2	linear to rotational . . . . .	30
4.5.3	Energy conversion location and method . . . . .	31
4.6	Combining sub solutions into total design. . . . .	31
4.6.1	Schematic design <i>I</i> , translating rotor . . . . .	32
4.6.2	Schematic design <i>II</i> , translating ratchets . . . . .	32
4.7	Comparison of schematic designs. . . . .	32
4.8	Further design choices based on schematic design . . . . .	33
4.8.1	Linear suspension and guidance . . . . .	33
4.8.2	Rectifier . . . . .	33
4.8.3	Combining sub-design . . . . .	35
<b>5</b>	<b>Model</b>	<b>37</b>
5.1	Dynamics . . . . .	37
5.2	Force in the system . . . . .	38
5.3	Losses in the system. . . . .	40
<b>6</b>	<b>Model analysis</b>	<b>41</b>
6.1	Mass . . . . .	41
6.2	Spring stiffness . . . . .	42
6.3	Radius of force . . . . .	43
6.4	Harvesting moment. . . . .	44

<b>7</b>	<b>Proof of concept</b>	<b>47</b>
7.1	Parameter choices . . . . .	47
7.1.1	Rotational mass . . . . .	47
7.1.2	Frame . . . . .	47
7.1.3	Linear guidance and spring . . . . .	47
7.1.4	Rectifier ratchet . . . . .	48
7.2	Ratchet wheel . . . . .	48
7.3	Total mechanism . . . . .	49
<b>8</b>	<b>Tests and Results</b>	<b>53</b>
8.1	Goal of testing . . . . .	53
8.2	Harmonic excitations . . . . .	53
8.2.1	input signal for harmonic excitations. . . . .	53
8.2.2	Results from harmonic tests . . . . .	54
8.2.3	Result interpretation . . . . .	55
8.2.4	Improved ratchet wheel performance . . . . .	56
8.3	Shock excitations . . . . .	57
8.3.1	results from shock tests . . . . .	57
8.3.2	Shock input result interpretation . . . . .	58
8.4	Bridge specific excitations . . . . .	58
8.5	Bridge specific excitations . . . . .	59
8.5.1	Gaussian envelope . . . . .	59
8.5.2	Bridge signal . . . . .	60
8.5.3	Stored energy from bridge specific excitations . . . . .	60
8.6	Test results . . . . .	60
<b>9</b>	<b>Conclusion and Discussion</b>	<b>61</b>
9.1	Discussion . . . . .	61
9.2	Conclusion . . . . .	61
9.2.1	Prototype . . . . .	61
9.2.2	Model . . . . .	62
9.2.3	Transduction . . . . .	62
9.2.4	Alternative application . . . . .	62

# Introduction

## 1.1. Energy harvesting

Energy harvesters subtract energy from their surroundings and convert this to a form of energy that can be used or stored, usually electrical energy. It is a form of renewable energy, but the term 'energy harvester' is often used in a context where energy output is very low, generally in the milliwatt range or lower. Energy can be harvested from different sources, such as photovoltaic energy, thermal energy, wind energy, radio frequency energy and mechanical vibration energy. Eventhough energy output is generally low for energy harvesters, they can be of great value. Combined with the developments in low power semiconductors, energy harvesters offer a possibility of self-sustaining devices. These devices nowadays often rely on power sources such as single-use batteries, rechargeable batteries that require periodic charging or a connection to a power net via cables.

Many examples can be found of applications that would benefit from energy harvesting. Not for all of these, suitable harvesters have been designed. In a comparative research into vibration energy harvesters and their performance T. W. Blad and Tolou, 2019 is concluded that lacking performance of vibration energy harvesters in the application fields of human wearables and remote sensing is the main hurdle in the widespread implementation.

Implementation of energy harvesters in these two fields could impact them greatly. Firstly considering application in human wearables. The amount of electrical devices people are carrying is increasing and many different types of products are available for consumers. Next to the smartphone most people use in daily life, one could think of smartwatches, wireless headphones, step counters and heartbeat sensors. Also in the medical field, wearable applications are used, such as pacemakers and blood glucose meters. All these devices run on batteries. Energy harvester could increase the battery lifetime of these products, reducing charging or replacement frequency. In the case of pacemakers, even surgeries can be avoided that are now required for the battery change T. Blad, 2021. Next to functional benefits, environmental benefits arise as well. Small, wearable electronics often rely on single-use batteries as a power source. Production and the waste of these batteries have a negative influence on the environment and contain toxic chemicals. Reduction of usage of these single-use batteries would therefore be beneficial and energy harvesters can play a role in this reduction.

Secondly, in remote sensing, energy harvesters can play a great role too. 'Remote sensing' covers a wide range of subjects where data is acquired from a distance. The category contains data acquisition methods like satellite imaging and radar technology by boats, but for energy harvesting application wireless sensor nodes are the mostly considered as an application area. Wireless sensor nodes comprise of a sensor, a power unit and often a data transmit and/or storage unit. These nodes can be equipped with a large variety of sensors and used in many different applications. One of these applications is monitoring the health of buildings and infrastructure, such as bridges. The next paragraph will elaborate on the use of these sensor nodes on bridges and what value energy harvesters can offer

in this application.

## 1.2. Energy harvesters in bridge health monitoring

Often bridges are maintained or inspected at pre-determined time intervals. Inspection of bridges is expensive, can be dangerous to the workers and can interfere with the availability of the bridge. Time based replacements of parts can also lead to extra costs or reduce usage time of the bridge as well. To reduce costs and increase safety of bridges and the people that work on them, sensors can be used to monitor health of bridges. Wireless sensor nodes can help to change from time based to necessity based inspection and maintenance. Sensor nodes with acceleration sensors are already used for this purpose, and research is still performed in this field Sarwar and Park, 2020. Acceleration sensors can be used to measure changes in stiffness of the bridge that can indicate damage. These sensors use little energy, and since the data can be transmitted with low energy usage, these sensors can run for years on a battery, without need for replacement. While this works fine for simple sensors, problems with power supply occur when more advance sensors are to be employed. Application of a of acoustic emissions sensors for bridge health monitoring is being researched. These sensors are passive sensors that are able to pick up high frequency ( $40kHz - 1MHz$ ) acoustic emissions that are caused by rapid discharge of localized internal energy in an elastic material such as crack propagations. The advantage of these type of sensors compared to acceleration sensors is that they can pickup damage in an earlier stage and that the location of the damage that develops in the bridge can be determined. Due to the high frequency( $40kHz - 1MHz$ ) and a low amplitude, the sensors to be very sensitive and have a high frequency sampling. As a result, the acoustic emission sensors require a lot more power to operate compared to acceleration sensor. Popular wireless sensors nodes for structural monitoring, use between  $300$  and  $450mW$  in active mode, but can also be placed in standby mode when measurements are not required, using as little as  $1mW$  Ledeczi et al., 2009.

Large scale implementation of these more advanced sensor nodes would be very costly when frequent battery replacements are required. Energy harvesters might offer a solution. While solar panels are a solution to reduce the dependency on batteries, there are some possible downsides. Firstly power wires will need to be run from the panels to the sensors. Secondly, for some bridges, aesthetics might be a reason not to implement solar panels. Although these shortcoming might be acceptable, alternatives methods can be considered. One of the alternatives is harvesting energy from the traffic induced vibrations in bridges. The company Kinergizer was asked to develop an energy harvester to locally power bridge sensors by means of traffic induced bridge vibrations.

This report will research the question whether a new type of vibration energy harvester, specifically designed for bridge excitations, can outperform current harvesters. In this report, a new type of vibration energy harvester for traffic induced bridge vibrations will be designed. To validate the working principle of the harvester, a proof of concept will be build. To achieve this, the following steps will be taken. Firstly, a detailed look into the bridge motion will be presented. Next, available research in energy harvesters will be reviewed to see whether suitable harvesters can be found in literature. This is followed by the design process of an energy harvester for the bridge deck vibrations. The design will then be approximated by a mathematical, analytical model. With the model, a basic parameter search will be done to find values for which the harvester should perform when subjected to given input accelerations. At last, a proof of concept will be build that resembles the system behaviour of the designed harvester. The proof of concept will be subjected to general signals the recorded bridge vibrations to see whether it works as intended.

# 2

## Ambient excitations in bridges

### 2.1. Introduction

Acceleration measurements a bridge in the Netherlands (the specific bridge is omitted for company reasons). These measurement will be used in this research to find a suitable design for an energy harvester. This bridge has been chosen because measurements have recently been performed here and thus data was readily available. For this early stage research measurements of one bridge are a good starting point for a feasibility study into harvesting energy from bridge vibrations. For wide applicability of the energy harvester multiple bridges should be measured to see if acceleration patterns are similar.

The vibrations in the dataset are traffic induced, no special events occurred during the measurements. Unfortunately, no specific observations of the traffic have been made during the test, so the type and properties of vehicles that caused the measured accelerations are not known. The bridge is situated in an industrial environment. As a consequence, the bridge is used mostly by trucks. This leads to the assumption that the higher accelerations in the dataset are caused by trucks passing the bridge.

The movement of the bridge is measured using accelerometers placed on various locations under the bridge deck. From the sensors, one is chosen that shows more often relatively high excitations compared to the other sensors on the same bridge during the same time. This dataset is chosen because the proof of concept prototype should at least work in relatively favorable conditions. If it performs well under these conditions, performance under lower intensity excitations can be researched later. The accelerations that are discussed and depicted in this chapter are perpendicular to the bridge deck, in the direction of gravity.

### 2.2. Measured excitations in the frequency domain

To start off the analysis of the ambient excitations, available frequencies of external excitations will be discussed. As the harvesters often comprise of a suspended mass and some sort of damper, this frequency of the excitations combined with the frequency response of the mass spring damper system results in the movement of the mass, shown in Figure 2.1. To start the analysis of the vibrations in the frequency domain, a spectrogram of the first ten minutes of the dataset is shown in Figure 2.2. In this figure the time is presented on the x-axis and frequencies are set on the y-axis. The power spectrum density, which represents how much energy is found in the signal per frequency over the time, are represented in colour. Red indicates that the frequency is represented more strongly in the vibrations, at around  $-30dB$ . Blue means that the frequency is found in lower amounts, depending on the shade between  $-70$  and  $-100dB$ . If a certain frequency would be found a lot in the dataset, due to, for example, an eigenfrequency or a periodic loading, horizontal lines would be visible in the spectrogram. In this spectrogram, mainly vertical lines can be observed. These vertical lines mean that a lot of frequencies are excited at the same moment in time. Comparing this data to Hertzian contact theory (Figure 2.3), similarities can be observed. During the moments of higher excitation level, most lower frequencies are can be found with similar intensities in the data, just as shown in the frequency plot of the Hertzian contact theory. In line with the theory, the intensity also starts to decay after a certain point (in the data

around  $50\text{Hz}$ ). This implies that the sensor is subject to shock-like excitations.

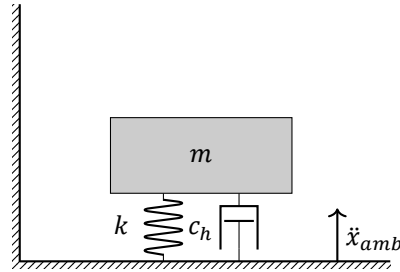


Figure 2.1: Free body diagram of a standard mass spring damper system, where  $m$  is the mass,  $k$  is the spring stiffness,  $c_h$  the damping by the transduction mechanism,  $\ddot{x}_{amb}$  the ambient accelerations.

Many energy harvesters in literature are resonance based. They only perform well at, or around, their eigenfrequency. The frequency spectrum that is found in the bridge does not seem suitable for a resonance based energy harvester. There are no dominant frequencies found in the signal. With a wide range of frequencies in the external excitations, the search for a non-resonant harvester seems logical, and the direction of research into a non-resonant harvester is pursued.

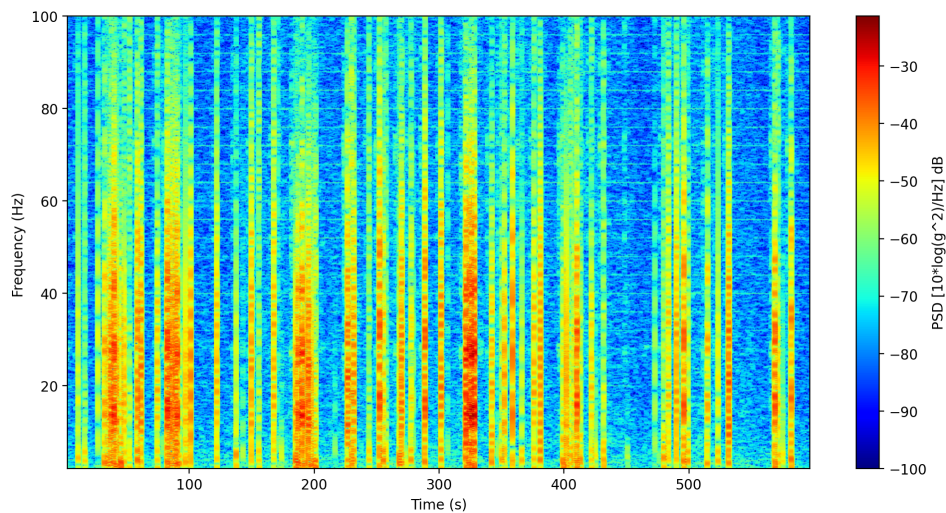


Figure 2.2: Spectrogram of the acceleration signal (made by MSc . Wetering, E.)

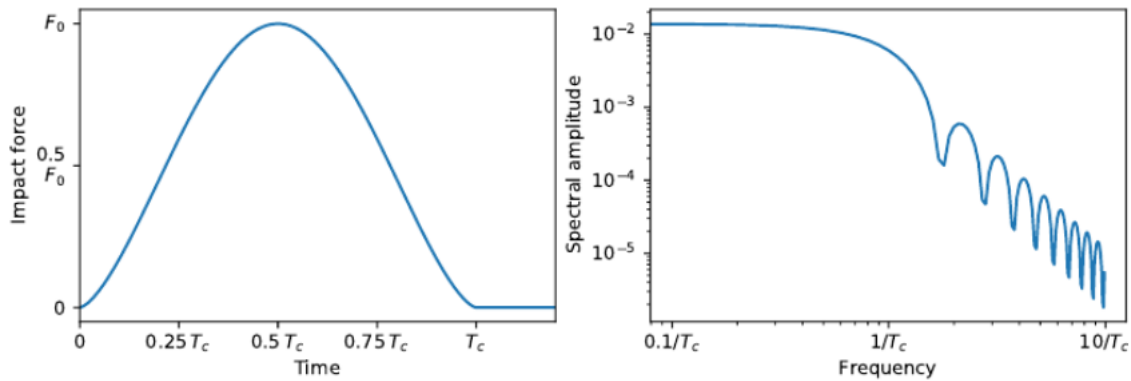


Figure 2.3: On the left the impact force vs. the impact time. On the right the frequency spectrum of impact contact between two elastic bodies.  $T_c$  is the impact time Kuehnert et al., 2020

## 2.3. Measured excitations in the time domain

For better understanding of the excitations that are present in the bridge, and for a non-resonant harvester, the time domain is very relevant. Therefore the accelerations in the time domain will be discussed in this section. Next to the accelerations, velocity and displacement can be of importance, especially when non-resonant harvesters are identified as design direction because they might depend on (respective) velocity and displacement. Velocity and displacement of the bridge in time domain will therefore be discussed as well.

The dataset is approximately an hour long and is measured with a sampling frequency of 1000 Hz and is displayed in Figure 2.4. In this plot time is displayed on the x-axis and acceleration in z-direction in  $m/s^2$ . In the figure can be observed that accelerations between peaks are around  $0m/s^2$ . During moments of higher acceleration values from  $0.2m/s^2$  are observed rather often and sporadically, decreasingly often with increasing acceleration value, up to  $5m/s$ , with a few outliers above  $5m/s^2$ .

A close up and a further close up of the close-up are shown respectively in Figure 2.5 and Figure 2.6 respectively. From the first close-up, with a duration of a little over two minutes, can be seen that there are short moments of increased activity. A short build up is observed, followed by maximum values in both positive and negative direction, and then a short period where the movement dampens out. Intervals between these moments of increased activity vary. Some are so close that a new burst occurs before the previous one has dampened out, while between other bursts, a period of little to no activity is visible.

Zooming in another time on the acceleration data, Figure 2.6 shows the accelerations over a time period of about 10 seconds. Here, the build up in the amplitude can be observed closer, showing that the build up in the amplitude is more gradual than the decline. When looking at the interval between the two bursts, there seems to be either always some vibrations present in the bridge or there is some noise in the data.

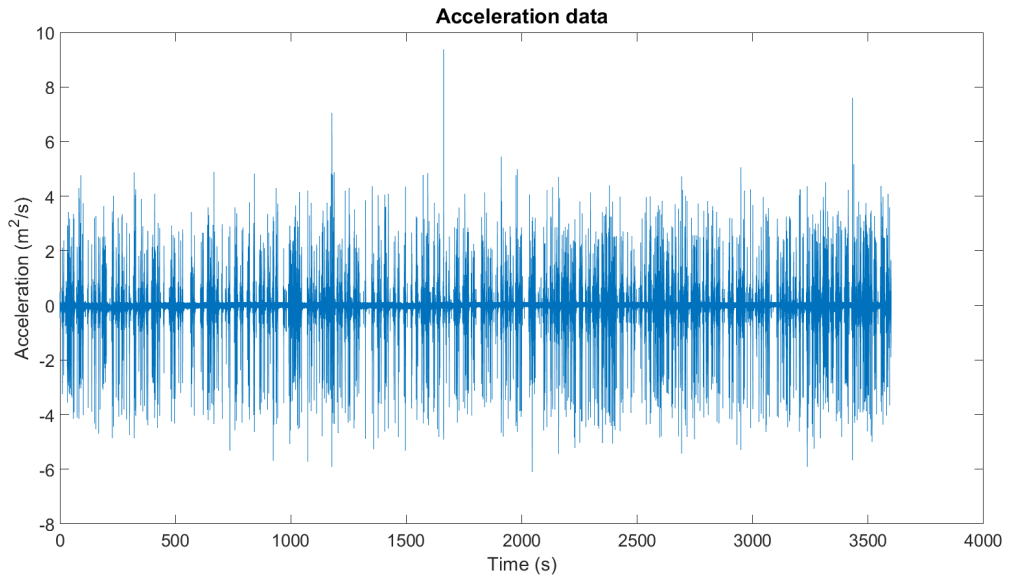


Figure 2.4: Acceleration data from the bridge

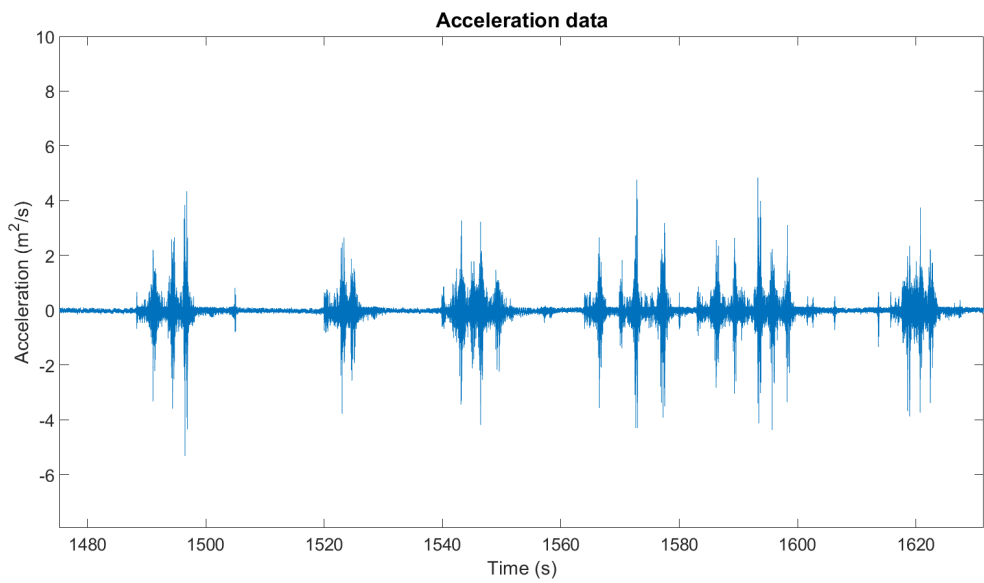


Figure 2.5: Acceleration data close up

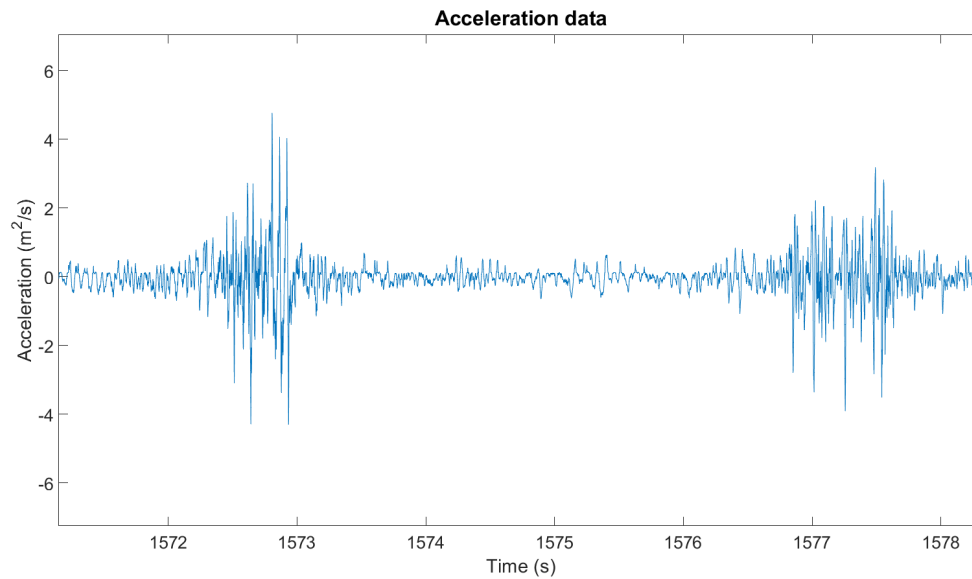


Figure 2.6: Acceleration data close up close up

The probability that at least some noise is present in the acceleration data becomes very likely when integrating the acceleration data to find the velocities of the bridge deck. Initial integration leads to the results displayed in Figure 2.7. This result is counter-intuitive. Based on the acceleration data, and the knowledge that a bridge under normal conditions stays approximately at the same height, one would not expect a negative speed for several minutes on end, especially at these magnitudes (reaching up to  $-30m/s^2$ ). More likely is that longer periods of negative and positive speed are caused by noise on the acceleration data. This is a well known drift that occurs when integrating acceleration data. To correct for this drift, a moving mean is subtracted from the velocity profile. The moving mean subtracts the average of each second from the data. This results in that vibrations at  $1Hz$  or lower are filtered from the data, integrated noise as well as actual vibrations that might be present in the bridge. When an energy harvester is designed that is displacement based, this method will need to be reconsidered. For velocity and acceleration based harvesters, these contribution of these low frequencies is expected to be so small that they would not influence the output of harvester. Choosing a smaller time window for the moving average would filter higher frequency vibrations, which might start to interfere with higher frequencies that could be designed for with a velocity or acceleration based harvesters. With a larger time window, drift remains present in the system.

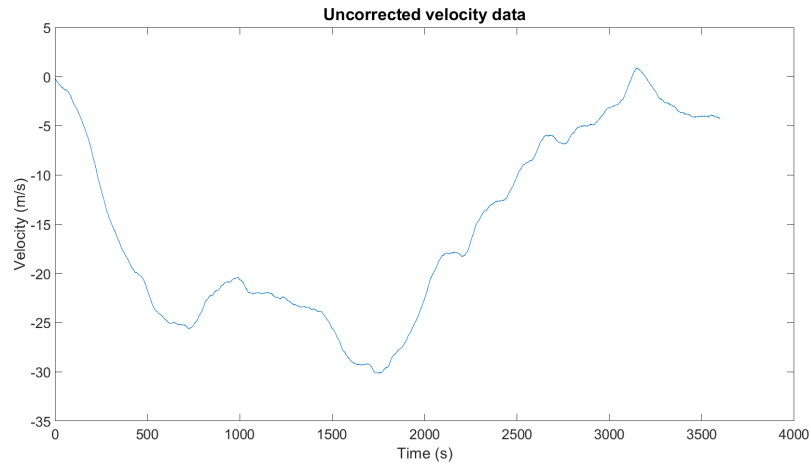


Figure 2.7: Velocity resulting from integrating acceleration data

After subtracting the moving mean, the velocity profile in figure 2.8 remains. In this plot speeds up to approximately  $.06m/s$  can be observed.

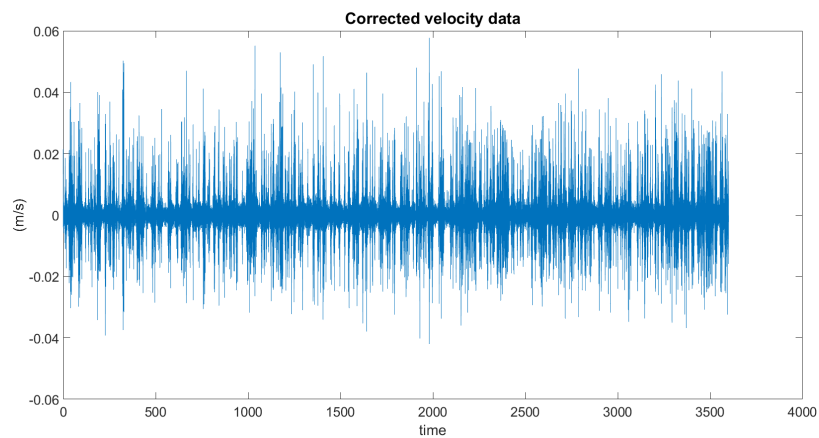


Figure 2.8: Velocity profile after subtracting a moving mean

To get some insight in the amplitudes of the movement, also the displacements are calculated. Again when integrating, this time the velocity instead of the accelerations, some drifts occur in the plot of the displacement. Using the same method as with the velocity profile, a moving mean is subtracted from the displacement. The found displacements are showed in Figure 2.9. In the figure can be observed that the bridges moves with a few maximal amplitudes around  $3mm$  during the measurement of an hour, but most displacement peaks are below  $1$  with sporadically some peaks till  $2mm$ .

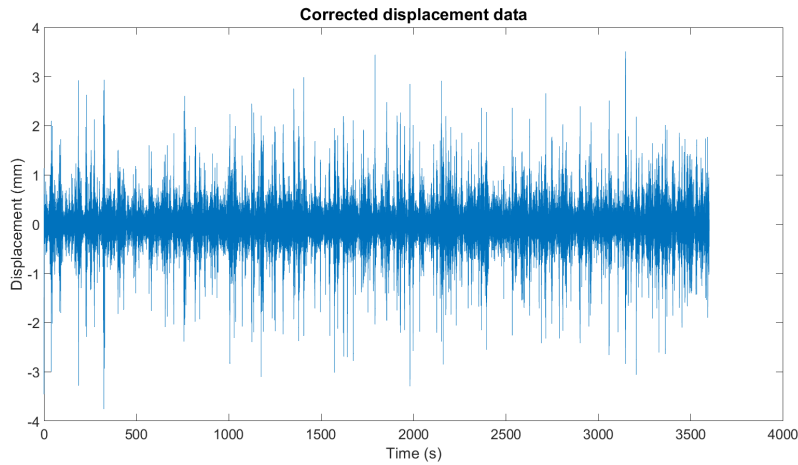


Figure 2.9: Displacement of the bridge

## 2.4. Conclusion on bridge vibrations

From the analysis of the bridge vibrations in the time domain, insight is obtained in how accelerations develop around peaks. These vibrations can be described as intermittent and shock-like. In the frequency analysis a wide range of frequencies is visible in the measured bridge vibrations, mainly in the lower parts of the frequency range (below 50 Hz). The intermittent nature of the vibrations leads to the idea that a non-resonant based energy harvest is a suitable design direction for this application. In the next chapter, a literature study will be presented into vibration energy harvesters for low frequency and non-harmonic excitation, to see if suitable energy harvesters can be found for bridge applications.



# 3

## Literature review

### 3.1. Introduction

In this chapter, a paper on the research into ultra-low frequency and non-harmonic excitations is presented, as this are the kind of excitations that are found in the bridge. In the chapter 2 these excitations will be discussed elaborately.

Multiple studies have been performed in the last few years to get a coherent overview of the research in energy harvesters. Where some have mostly focused on categorizing Maamer et al., 2019, others have made quantitative comparisons between different harvesters (Talib et al., 2019). As discussed in a paper by T. W. Blad and Tolou, 2019, a simple quantitative comparison of power output or power density does not suffice for determining relative efficiency between harvesters. An alternative method to account for different designs is proposed. This method takes into account a lot of characteristics of an energy harvester, such as volume, mass, motion range, output power and bandwidth, to determine performance compared to other harvesters.

The operating frequency and bandwidth of harvesters has been an important part of the research field. Most harvesters are resonant based (He et al., 2019). The eigenfrequency of the harvester is tuned to a specific, harmonic frequency that is dominantly available in the environment where it is placed. Figure 3.1 shows some examples of vibration sources. Earlier studies have looked into frequency tuning of vibration harvesters (S. W. Ibrahim and Ali, 2012). Performance of resonant based harvesters quickly reduces when the excitation frequency starts to differentiate from the resonance frequency. This narrow bandwidth was identified as a large drawback in energy harvester design and studies looked into broadening the operation bandwidth (Salem et al., 2021, Jackson et al., 2015).

To evaluate the performance of an energy harvester, a frequency sweep is usually used to determine power output and operating bandwidth. In current research into energy harvesters, often mentioned application fields in literature are human wearables and remote sensing (Pillatsch et al., 2012, W. Jiang et al., 2021). As Figure 3.1 shows, human walking and motion takes place in ultra low frequency regions. As concluded in a recent review of the field T. W. Blad and Tolou, 2019, bad performance of energy harvesters at low frequencies is a very important cause of limited implementation of energy harvesters in practise. Excitation profiles in remote sensing differ per application. For bridges we see a non-harmonic and low frequency excitation profile (Galchev et al., 2011). Also, resonance can usually not be used since there no predetermined, constant frequency vibration in the system. To evaluate applicability for harvesters for these often mentioned applications and other applications with non-harmonic excitations, the review of the performance of harvesters should consider transient behaviour and energy output under non-resonant excitation conditions.

In this paper an overview will be given of current available types of harvesters for ultra-low frequency and non-harmonic excitations. In section 3.3.1 this overview can be found. Before presenting the overview, some more detail of how energy harvesters work and in what way the classes are determined

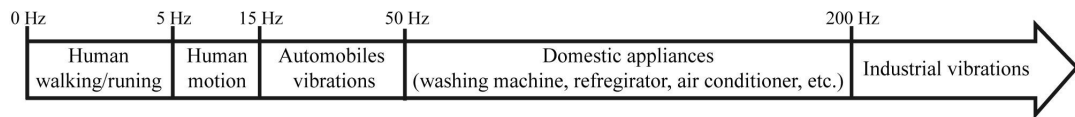


Figure 3.1: Vibration sources and their frequency region. Maamer et al., 2019

is presented in section 3.2. Section 3.4 will present some results from literature that show transient and non-resonant behaviour of energy harvesters. In section 3.5 will be discussed if the results from literature allow for deducing some dominant development directions for the often mentioned application fields for energy harvester, human wearables and remote sensing.

The results and information in this paper are found by searching for the following keywords in google and google scholar: Energy harvester, Low frequency energy harvester, Ultra low frequency energy harvester, Vibration energy harvester, Non-resonant energy harvester, Shock energy harvester, Rotational energy harvester, Multi-modal vibration energy harvester, Fluid energy harvester, Bi-stable energy, Tri-stable energy harvester, Multistable energy harvester, Free moving mass harvester, Energy harvester review.

## 3.2. Mechanisms in harvesters

In vibration energy harvesters we can identify two systems that are generally present, the power takeoff mechanism and the transduction mechanism.

### 3.2.1. Power takeoff mechanism

The power takeoff mechanism absorbs energy from external sources. This mechanism consists of a mass that is accelerated by the external vibrations. When the mass is moving, the kinetic energy of the mass can be converted into electric energy. The transducing mechanism is responsible for this conversion. For a simple example we can look at figure 3.3. In this figure, the by a flexure suspended mass will start to oscillate when the ground moves, this is the power takeoff mechanism.

### 3.2.2. Transducing mechanism

The piezo layer (Figure 3.3) will convert movement of the power takeoff mechanism and convert it into electric energy, the transducing mechanism in this example. In the current vibration energy harvesters most transducing mechanisms are electromagnetic (EM) or piezo electric (PE) based, multiple examples of energy harvesters with EM and PE transducing mechanism can be found in the next section (3.3.1). Harvesters with other transducing mechanisms can be found such as triboelectric A. Ibrahim et al., 2020 or electrostatic Zhang et al., 2018 transducing mechanisms but these are less common.

## 3.3. Classification

A wide variety of setups have been designed to improve energy production and to the behaviour of the harvester under different excitation patterns. To get a better overview of what kind of harvesters have been researched, the harvesters will be grouped by working mechanism and examples will be presented per group with an explanation of the concept of the harvester.

Harvesters found in literature have been divided into two larger classes, suspended and non-suspended systems, with three sub classes each (Figure 3.4. In the following section (3.3.1), the classes will be described and examples of available harvesters are given.

### 3.3.1. Classes

Division of the power takeoff mechanisms is not as trivial as the transducing mechanisms. As proposed in an earlier review by Covaci and Gontean, 2020, we can identify two larger groups in this ultra-low frequency region.

- 1) Non-suspended systems (Figure 3.5)
- 2) Suspended systems (Figure 3.6)

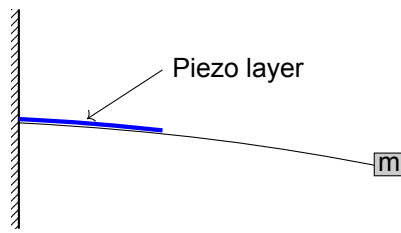


Figure 3.3: Simple energy harvester

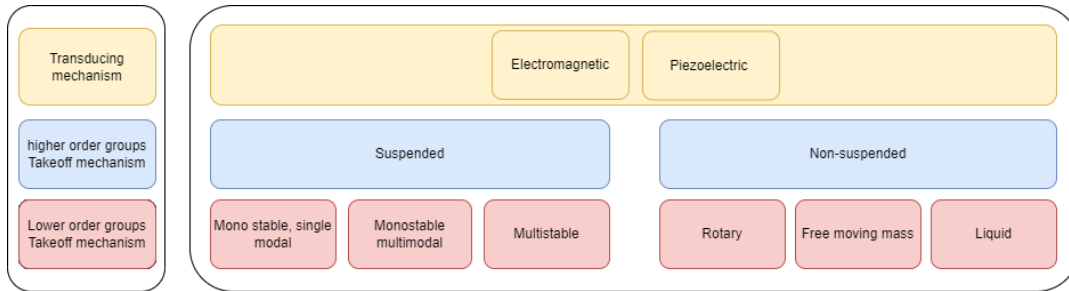


Figure 3.4: Classification of ultra-low frequency energy harvester

Since the research field is ever expanding due to the high interest in human wearables and remote sensors without battery dependence and a wide variety of EH is being researched in the ultra-low frequency harvesting field, a further division within these two larger groups is proposed (Figure 3.4).

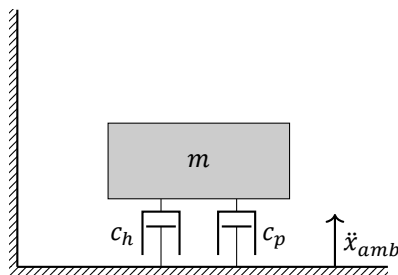


Figure 3.5: Free body diagram of a non-suspended harvester, where  $c_p$  is the parasitic damping,  $c_h$  the damping by the transduction mechanism,  $\ddot{x}_{amb}$  the ambient accelerations that enter the system.

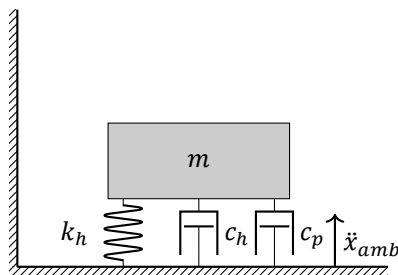


Figure 3.6: Free body diagram of a suspended harvester, where  $k_h$  is the the stiffness in the harvester,  $c_p$  the parasitic damping,  $c_h$  the damping by the transduction mechanism,  $\ddot{x}_{amb}$  the ambient accelerations that enter the system.

### 3.3.2. Non-suspended EH

In this classification we use the term non-suspended for mechanism that do not suspend a mass with springs, flexures or magnets. A wide variety of harvesters fall in this category. For better understanding of the currently available harvesters, a further division can be helpful. For the non-suspended EH's four smaller subsets can be identified:

- Rotary systems
- Free moving mass
- Liquid based systems

A further description of these categories with examples will be presented next.

#### Rotary systems

In rotary systems, the proof mass has a rotational degree of freedom. When excited by external vibrations, the mass acquires a rotational speed. Whilst the proof mass moves in a rotational manner, the excitation doesn't have to be. Gears or an eccentrically placed mass can convert linear into rotational motion (Fu et al., 2021). This paper shows that, when looking at non-resonant, linear excitations, rotational harvesters have the same theoretical maximum as their linear equivalents (Yeatman, 2008). Rotary systems for energy harvesting have been around for a long time. A well known example are self-winding watches, that have been in use for decades. Although other mechanism are used, the more common self winding mechanism consisted of a eccentric mass attached to a rotational spring and was used to automatically wind wristwatches (Figure 3.7a). Where the self winding watch mechanisms convert kinetic energy into potential energy in the spring, similar mechanisms have been researched that convert the potential energy into electric energy. Studies consider EM (Figure 3.7b), PE (Figure 3.7c), or a combination of the two transducing mechanisms (Figure 3.7d) with different kinds of plucking mechanism.

Rotational harvesters are not limited to the well known eccentric mass example. In literature we see other examples of rotational harvesters such as the harvester by Luo et al., 2020. This paper also presents energy production of a single impulse, where most papers only present results of a frequency sweep of harmonic inputs, and shows high efficiency at low ( $\ll 1Hz$ ) frequencies. Figure 3.8 shows the working mechanism of this harvester. The harvester converts a compression force into rotational movement of a mass. Kinetic energy of the mass is converted into electric energy by an EM transducing mechanism. The paper shows high efficiency percentages in this last energy conversion, up to 97.2%.

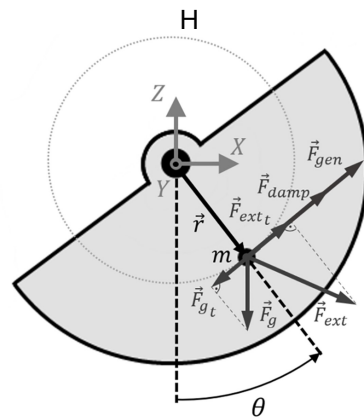
#### Free moving mass

Free moving mass systems are systems that make use of a moving mass that is not restricted to a single DoF. Here the takeoff mechanism often consist of a ball or a disk that can freely move through space within the harvester. In Figure 3.9 an example is shown. In this harvester, the proof mass is a rolling ball. The impact from the mass on the cage is used as an frequency-up conversion, where vibrations in the cage are then used as input vibrations for the transducing mechanism.

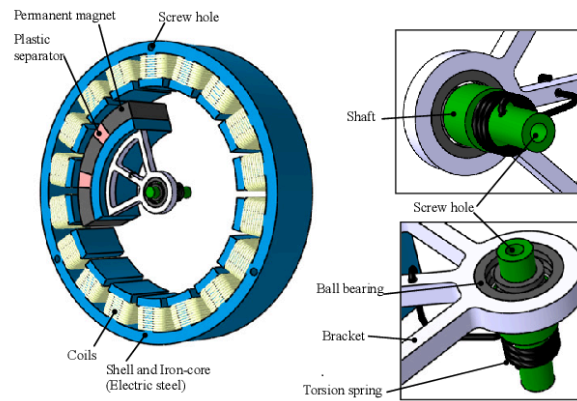
Free moving mass harvesters intuitively allow for harvesting in more than one direction and are indeed are used in 2D and 3D. In Figure 3.10 an example of such an 2D harvester is displayed. In this one, energy is produced during the movement of the proof mass itself instead of the impact of the mass as is the 1D example (Figure 3.9).

#### Liquid based system

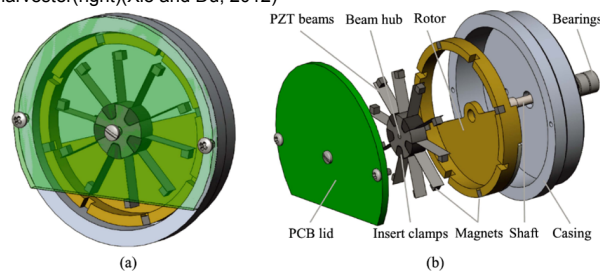
A harvester that uses ferrofluid as an takeoff mechanism was investigated by Bibo et al., 2012. In this setup, permanent magnets are placed in close proximity such that the fluid is polarized (Figure 3.11). When the fluid is excited by vibrations, it will move and changes in the magnetic field are converted into energy by the nearby situated coils.



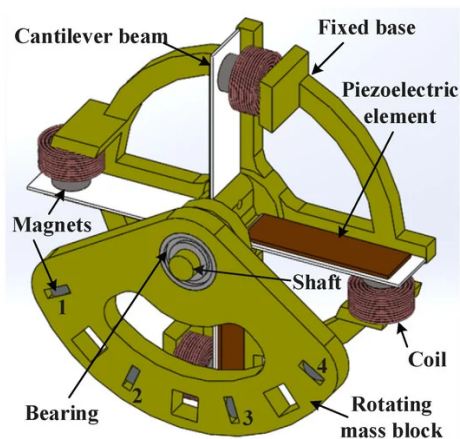
(a) Eccentric mass



(b) EM eccentric rotational energy harvester(right)(Xie and Du, 2012)



(c) Eccentric mass PE(Xue et al., 2018)



(d) Eccentric mass EM and PE combination(Shi et al., 2020)

Figure 3.7: Eccentric mass harvesters

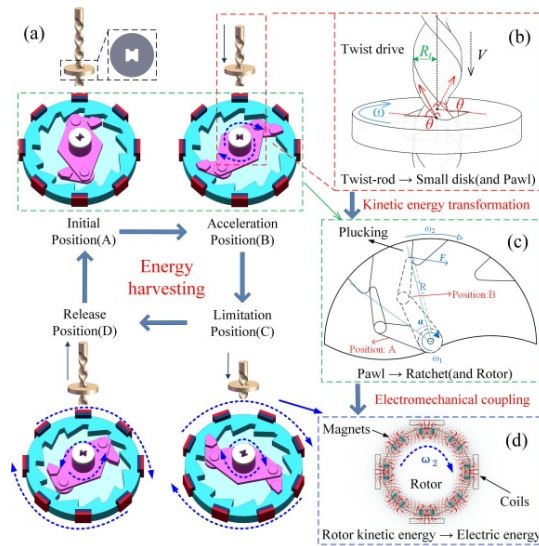


Figure 3.8: Rotational harvester (Luo et al., 2020)

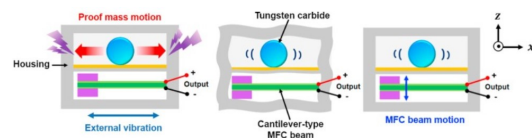


Figure 3.9: Free moving mass harvester (Ju and Ji, 2018)

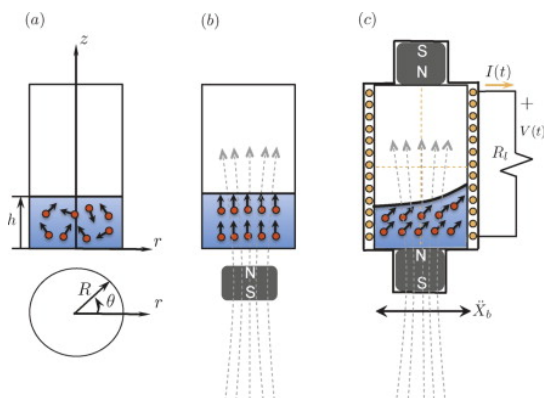


Figure 3.11: Liquid based harvester (Bibo et al., 2012)

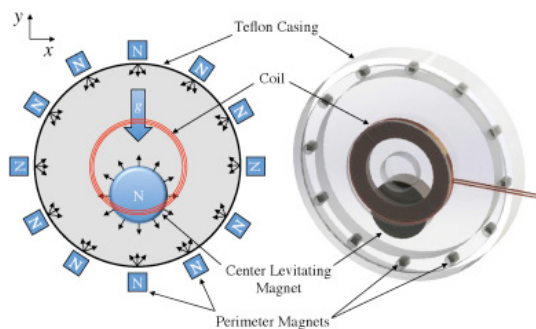


Figure 3.10: Free moving mass harvester (n DGutierrez et al., 2015)

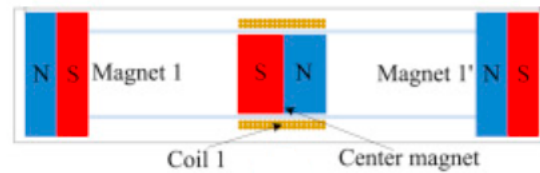


Figure 3.13: Monostable suspended magnet(Fan et al., 2019)

### 3.3.3. Suspended systems

In the suspended systems class we see a wide variety of harvesters and papers. These harvesters show more resemblance in working mechanism with higher frequency energy harvesters. Just like in the higher frequency harvesters, the takeoff mechanism in these harvesters operates at its eigenfrequency. Energy is harvested during the stroke or at endstops with impact or a plucking mechanism.

#### Single mode, monostable

In this category we see the most simple harvesters. These (takeoff) mechanisms often consist of a single cantilever or a magnet suspended with springs or other magnets. In the early research phase of the ultra low frequency domain, the main focus was to tune the harvesters to specific (low) working frequencies. The research has developed into the direction of widening the operating bandwidth (Salem et al., 2021, Jackson et al., 2015).

In a simple linear cantilever system without endstops (Figure 3.12) the system can be described by the formula:

$$M\ddot{u} + C\dot{u} + Ku = F_{ext} \quad (3.1)$$

Where the external force ( $F_{ext}$ ) is caused by movement of the base of the cantilever.  $K$  is the stiffness matrix of the system.  $C$  is the damping matrix that is present in the system. This includes the transduction, this can be modeled as a damping, but also the parasitic damping that will always be present in a system.  $M$  is the mass matrix.

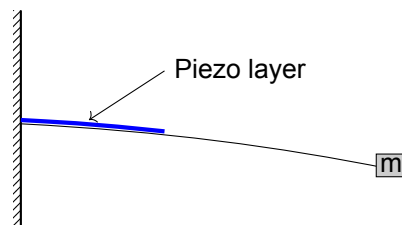


Figure 3.12: monostable cantilever

Many harvesters have been based on this simple mechanism. In literature, alterations of and additions to the simple systems have been implemented in a search for improved performance. One example is different kinds of endstops (soft, hard), limiting the maximum vibration amplitude of the cantilever. Another one is altering the stiffness by replacing the mass with a magnet and placing another magnet in the near proximity (Tang and Yang, 2012). In the ultra low frequency energy harvesting, a frequency-up conversion in a cantilever system is examined. In a frequency-up conversion, the takeoff mechanism and the transduction mechanism are separated. The cantilever in the picture would only function as takeoff mechanism, without the piezo layer and activates the transduction mechanism with an impact or plucking at the end or during the stroke. The transduction mechanism, which could be for example an other cantilever or a suspended magnet, will then start oscillating at a higher frequency than the takeoff mechanism and the transduction will take place in this higher frequency subsystem. Another simple system that is researched in different form, although maybe less than the cantilever system, is a levitation magnet (Figure 3.13). Next to this most simple setup, also for example setups with frequency-up methods are researched with suspended magnets as endstops, where the transductions takes place (Galchev et al., 2011, Halim et al., 2015).

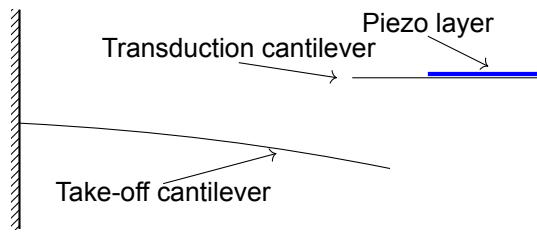


Figure 3.14: Frequency up conversion. The take-off cantilever will start to oscillate at a low frequency by ambient vibrations. During the low frequency oscillations, the take-off cantilever impacts on the transduction cantilever, which will start to oscillate at its (high) eigenfrequency. A piezo will convert the movement of the cantilever into electric energy

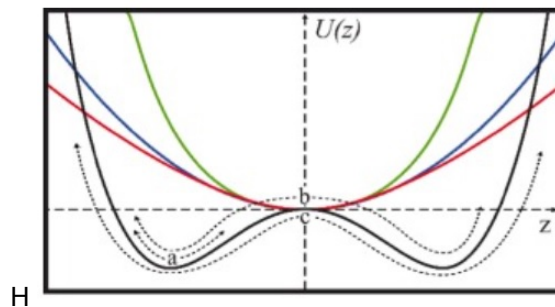


Figure 3.15: Double well potential energy(black line) and three oscillation types (a,b,c)(Maamer et al., 2019)

### Multistable

In multi-stable systems a single DOF system has multiple stable positions and can exhibit multiple oscillation modes. Examples of common bistable cantilevers can be found in Fig 3.16. In Fig. 3.15. an example of the potential energy versus deflection for a bi-stable system is shown, the famous Duffing type oscillator. The two wells(lowest points) in the graph represent the stable equilibria. This bi-stable oscillator can show three oscillation types(Fig. 3.15). For small excitations the systems behaves similar to a simple monostable system around one of the stable equilibrium positions. For higher amplitude or acceleration excitations, chaotic behaviour can be observed. This bi-stable system should be able to produce more power under similar conditions than a mono-stable system, according to research where they theoretically compared the two systems with similar characteristics(Zou et al., 2016). Higher order systems, such as tristable or quad-stable and even higher orders, have also been researched. These papers report less need for tuning and thus wider application possibilities. In the higher order systems, the walls between different wells can be smaller, resulting in more jumps between wells, which leads to larger amplitude vibrations and more energy production (J. Jiang et al., 2021)

### Multimodal, mono stable

In the pursuit of acquiring higher bandwidths at low frequencies, multi-modal takeoff mechanisms have been researched. These mechanisms have been designed such that several eigenmodes can be found in the ultra low frequency region. By implementing several modes with different eigenfrequencies, a wider range of excitations can be converted. An example of the concept can be found in Figure 3.17. Although the operating frequencies in this example are much higher, they nicely depict the idea on how multiple modes reach a higher bandwidth.

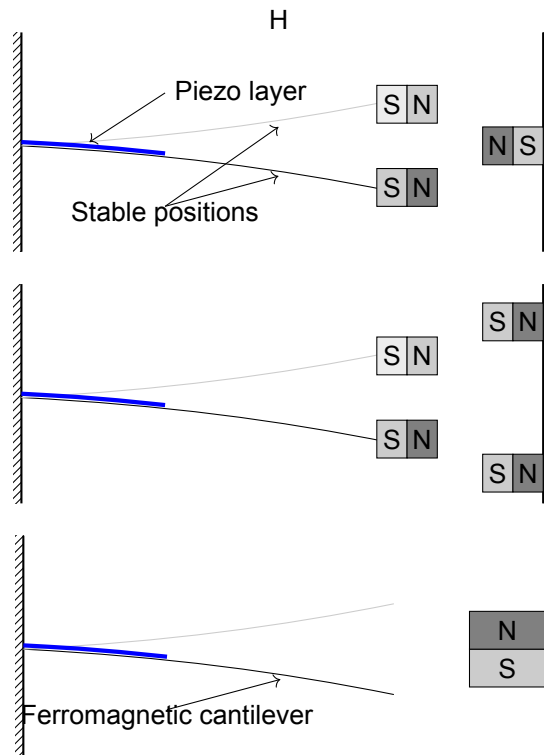


Figure 3.16: Common bi-stable cantilevers(1.Repulsion 2. Attraction 3.Ferromagnetic cantilever), recreated from Maamer et al., 2019

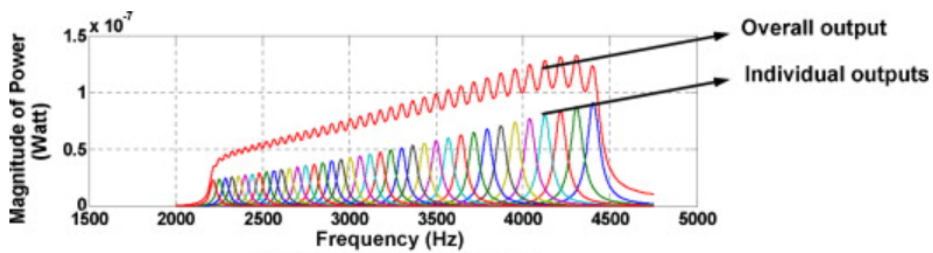


Figure 3.17: Combining multiple eigenmodes for wider bandwidth Sari et al., 2008

### 3.4. Results

Performance of energy harvesters that are tested under non-resonant conditions, such as shock-like or impulse excitations, or output that shows a transient response to harmonic/low frequency excitations are shown in the following table 3.1. Since output is highly dependent on the test conditions, input signals for the transient performance, dimensions and output are given for comparison. The input given in the table is only the input where a transient response and or result is given, some of the harvesters are also tested for harmonic, frequency dependent results, these test methods are not given in this table.

Table 3.1: Energy harvesters, tested under shock-like or impulse excitations, or output that shows a transient response to harmonic/low frequency excitations. In the output column, some papers only show a voltage output ( $V_{out}$ ) plot for the presented test method. (\*:data is read from graph or combined from data in the paper)

Paper	Class	Test method	Frequency	Acceleration	Output
Galchev et al., 2011	Suspended, single mode	Sinusoidal	2Hz	$0.55m/s^2$	$0.56\mu W$
		Sinusoidal Installed on a bridge	10Hz [-]	$0.55m/s^2$ [-]	$0.60\mu W$ $0.46-0.74\mu W$
He et al., 2019	Suspended, single mode	tested periodically with a stroke length of 2mm by having a (60kg) person step on it	0.47Hz	[-]	$2.72\mu W$
		tested periodically with a stroke length of 5mm by having a person step on it	0.95Hz	[-]	$48.18\mu W$
		tested periodically with a stroke length of 5mm by having a person step on it	1.41Hz	[-]	$91.18\mu W$
		tested periodically with a stroke length of 5mm by having a person step on it	1.81Hz	[-]	$134.2\mu W$
Hadas et al., 2012	Suspended, single mode	behaviour after initial displacement	[-]	[-]	$V_{out}$ plot
		Mechanical shock by shaker with an amplitude of 3mm	.5Hz	12, 5g	RMS 5.1V
		Mechanical shock by shaker with an amplitude of 3mm	2Hz	12, 5g	RMS 8V
		Mechanical shock by shaker with an amplitude of 3mm	3Hz	12, 5g	RMS 8.1V
		Mechanical shock by shaker with an amplitude of 3mm	4Hz	12, 5g	RMS 3.5V
		Mechanical shock by shaker with an amplitude of 3mm	Random	12, 5g	$V_{out}$ plot
Luo et al., 2020	Free moving mass, rotational	Driven by compression from a crank-slider	0.25Hz	[-]	RMS 2mV
		Driven by compression from a crank-slider	0.44Hz	[-]	RMS 2mV
		Driven by compression from a crank-slider	0.84Hz	[-]	RMS 2mV
		Driven by compression from a crank-slider	2.82Hz	[-]	RMS 2mV
		incorporated in a shoe, moving at a speed of 1km/h on a treadmill	[-]	[-]	$3mW^*$
		incorporated in a shoe, moving at a speed of 3km/h on a treadmill	[-]	[-]	$20mW^*$
		incorporated in a shoe, moving at a speed of 5km/h on a treadmill	[-]	[-]	$47mW^*$

		incorporated in a shoe, moving at a speed of $7km/h$ on a treadmill	[-]	[-]	$66mW^*$
		incorporated in a shoe, moving at a speed of $9km/h$ on a treadmill	[-]	[-]	$85mW$
Ylli et al., 2015	Suspended, single mode	Tested installed in a shoe, worn at running speed of $4km/h$ by 2 different persons(p1 and p2 in output column)	[-]	$18g$	$1.3mW(p1)^*$ , $1.3mW(p2)^*$
		Tested installed in a shoe, worn at running speed of $6km/h$ by 2 different persons	[-]	$18g$	$3.1mW(p1)^*$ , $3.6mW(p2)^*$
		Tested installed in a shoe, worn at running speed of $8km/h$ by 2 different persons	[-]	$18g$	$2.6mW(p1)^*$ , $2.2mW(p2)^*$
		Tested installed in a shoe, worn at running speed of $10km/h$ by 2 different persons	[-]	$18g$	$2.9mW(p1)^*$ , $2.9mW(p2)^*$
W. Jiang et al., 2021	Suspended, single mode	Tested under shock accelerations	single shock	$1.81g$	$V_{out}$ plot
		Tested under shock accelerations installed on shoe	single shock	$3.64g$	$V_{out}$ plot
		Tested under shock accelerations installed on shoe	single shock	$5.52g$	$V_{out}$ plot
		Tested under shock accelerations installed on shoe	single shock	$7.20g$	$V_{out}$ plot
		Tested under shock accelerations installed on shoe	1 Hz	$4g$	$0.1mW$ average in 5 seconds
Wang et al., 2016	Free moving mass, rotational	Harvester incorporated in speed bump, ran over by $950kg$ at speeds from 2 – $15mph$ )	single run	[-]	65 till $120J^*$
		Harvester incorporated in speed bump, ran over by $1527kg$ at speeds from 2 – $15mph$ )	single run	[-]	119 till $160J^*$
		Harvester incorporated in speed bump, ran over by $2210kg$ at speeds from 2 – $15mph$ )	single run	[-]	155 till $220J^*$
Bonisoli et al., 2017	Suspended, single mode	Slow jogging condition is measured and recreated on shaker	$1.5Hz$	peaks at $20g$	$0.54mW$
Yang et al., 2019	Free moving mass, rotational	Tested in the lab with sinusoidal input with $10mm$ amplitude	$1Hz$	$2.5 \cdot 10^{-4}m/s^{2*}$	$0.01W^*$

Tested in the lab with sinusoidal input with 10mm amplitude	1.5Hz	5.7 $10^{-4}m/s^2*$	*	0.07W*
Tested in the lab with sinusoidal input with 10mm amplitude	2Hz	1.0 $10^{-3}m/s^2*$	*	0.23W*
Tested in the lab with sinusoidal input with 10mm amplitude	2.5Hz	1.6 $10^{-3}m/s^2*$	*	0.49W*
Tested installed on bike while riding over a speed bump with a speed of 2m/s	single run	[-]		0.313W (peak)

### 3.5. Discussion

A few observations can be made from looking at Table 3.1. First of all, a lot of different testing methods can be found here. Harvesters for ultra-low and non-harmonic excitations are often tested in their intended application environment. As mentioned in section 3.1, energy harvester designs that focus on sinusoidal/harmonic inputs, performance is often evaluated by doing a frequency sweep. Even under these relative similar testing conditions, a rather advanced method is developed for performance comparison. This implies that performance comparison of harvesters under completely different test conditions is even more complex.

That comparison between these harvesters is far from trivial is supported by a second observation that can be made. For the same harvester in a similar setup, the output of the harvester can differ a lot depending on the input. For example a different person using the harvester, different speed or weight of vehicle running over the harvester or excitation at a different frequency leads to large differences in results. When a harvester is tested in relatively similar conditions, an attempt at comparison can be made. This is done by Bonisoli et al., 2017, where a harvester is installed in a shoe. As soon as performance from harvesters is in the same order of magnitude, comparison between papers could be rendered useless. Differences in test setup (test subjects weight, step or speed), could have such a large impact that better performance can't be concluded from higher output energy.

A third observation is that the power output is often a few  $mW$  or less. Some of these harvesters are designed for human wearables and are thus made within certain design parameters, such that a person could easily transport it.

### 3.6. Conclusion

Current performance tests for non-periodic harvesters are often too different to compare harvesters from different papers. A more standardised performance measurement method for non-resonant harvesters could decrease this problem. Especially research into harvesters in the field of remote sensing, where excitations can differ per location, could benefit from a standardised test. Comparison between harvesters will be more straightforward. Better designs will be easier to identify because power output can be compared for similar input between papers. Also, when designing a harvester for a new application, appropriate harvesters can be found by evaluating the (expected) vibrations in the intended environment and see which harvester perform well under such conditions. An appropriate test method would need to be developed that provides data for a wide variety of possible applications of non-periodic vibrations harvester.

While such testing protocols have not yet been implemented, extrapolation of results will need to be done when the results in the test do not resemble the test inputs from previous research. Comparing the results and working methods from vibration energy harvester to the bridge vibrations, some observations can be made. Many designs are resonant based. As is concluded in the chapter about the bridge vibrations, due to the intermittent character of the vibrations, resonant based harvesters are expected to achieve low energy output. Some of the harvesters perform well under intermittent inputs. These harvesters (Wang et al., 2016) make use of an secondary external mass that is not part of the harvester and moves relative to the ground such as displayed in figure 3.18.

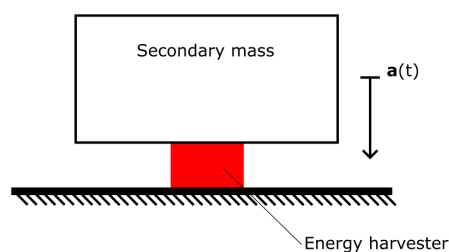


Figure 3.18: Harvester making use of a secondary mass that is accelerated with respect to the ground



# 4

## Design

In this chapter a design for an energy harvester will be generated. The goal of this design of the harvester is to explore the possibility of using a vibration energy harvester for application on bridges. One design will be chosen based on first principles. Different methods are available to generate a new design. For the design of a power takeoff mechanism, a main design direction will be chosen from the literature research paper in Chapter 3. Within this design direction, a design space will be identified by determining which sub-functions are present in the harvester. For each of these sub-functions, design solutions will be presented and evaluated for the applicability of the harvester in the intended use situation.

### 4.1. Main design direction

For the main design direction of the energy harvester for bridge application, three main directions are considered (Figure 4.1). The first one is an harvester that harvests energy from the movement between the movement of the bridge deck and the a support point (a pillar or the ground). The second one is a harvester that harvests energy from the speed and/or the gravitational force from the passing vehicles. The third one is an inertial harvester that only uses bridge vibrations as ground accelerations without external masses such as vehicles.

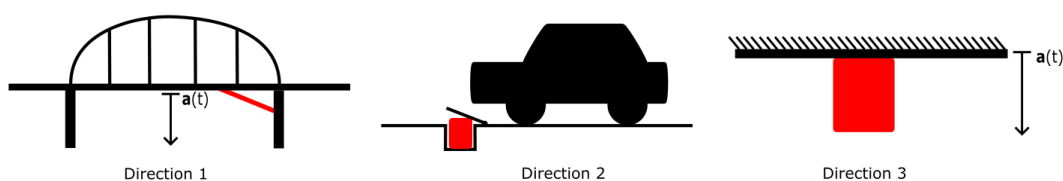


Figure 4.1: Main design directions 1, 2 and 3. In red the energy harvester for bridge applications

Considering the first option: Due to large mass of the bridge, large forces will arise when the bridge deck moves with respect to a ground. This could result in high energy output. On the downside, when applying this concept in retrofitting, the bridge will endure the same but opposite large forces, which it is not build for. The harvester will change the structure of the bridge. This, and the fact that bridge can differ a lot in type of structure, makes that for each bridge a different harvester would need to be designed that takes into account the design of the bridge and the strength. This would limit scalability of harvester application.

Considering the second option: Using the displacement of the vehicles on the bridge can be used to

generate a force on a harvester, such as is done in research (Wang et al., 2016), where an energy harvester uses a speed bump to create a compressive force which is used to accelerate a proof mass. While at low speed environments for vehicles placing a speed bump can be an appropriate solution. At bridges, however, driving speed is generally higher, and speed bumps will cause discomfort for users of the bridge.

Considering the third option: This type of energy harvester has the advantage that it is versatile. It can be installed easily and does not have to be designed specifically for different bridges. The harvester does not hinder traffic that uses the bridge. The downside of this option is that energy output is expected to be relatively low compared to the other two options since this harvester only uses the vibrations from the bridge as input, which have been identified to be intermittent, low frequency and low accelerations, where the other options use a force between two external bodies.

While the low energy output might be a problem, the third option is chosen because the problems with the first two harvesters, limitations in scalability and driver discomfort, are considered significant and should be avoided if possible. In this research an inertial harvester will be designed.

From the literature study it is concluded that there are energy harvesters that perform well under intermittent excitation, but these require a secondary body. Since the vibrations are identified to not be particularly suited for resonant based harvesters, because no dominant vibrations are observed in the signal, the decision is made to design a non-resonant based harvester.

## 4.2. Design method

As discussed in the literature study, energy harvesters can be divided into two subsystems, the takeoff system and the transduction system (red and blue encircled in Figure 4.2). The function of the takeoff system is to subtract energy from the environment. The transduction system converts this subtracted energy into electrical energy. The design will be focused on the power takeoff part of the harvester. The aim is to maximize the energy in the power output for bridge-like excitations. To evaluate the performance of the harvester, it will be subjected to harmonic excitations as well as different shapes of non-harmonic excitations. More details of these test excitations and the results will be presented in Chapter 8.

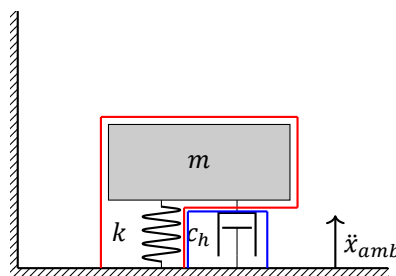


Figure 4.2: A standard mass spring damper system with the takeoff part of the mechanism system encircled in blue and the transduction part encircled in red. In the figure  $m$  is the mass,  $k$  is the spring stiffness,  $c_h$  the damping by the transduction mechanism,  $\ddot{x}_{amb}$  the ambient accelerations.

Designing an inertial vibration energy harvester for bridge excitations offers some challenges and opportunities compared to available inertial harvesters, that are often designed for human motion. One of the opportunities is a result of the high weight of the bridge. This means that a proof mass with a higher weight can be used compared to energy harvesters for human wearables without having a significant effect on the movement. Additionally, the harvester is placed on a stationary object (the bridge), and does not need to be transported, such as a harvester in/on a vehicle or worn by a human, so there are little restrictions on the weight. Finally, there is a plenty of space, so there are no strict limitations to the size. A disadvantage is that the accelerations, velocities and displacements are relatively low, thus a larger mass is needed to attain a significant force acting on the system.

Within the harvesters that are covered in the literature review, one type shows behaviour that seems to perform well with the bridge excitations that have been discussed in the previous Chapter (2). A centric, rotational harvester from research (Luo et al., 2020) shows that it performs under a single compression, but also after compressions closer together in time, where the mass is accelerated while it is still rotating from an earlier excitation. This property can also be used for bridge excitations. These excitations are intermittent, with short acceleration peaks. Due to the rotational inertia, the harvester can harvest energy for a longer duration. The harvester in this research uses compression force between an external body and the ground to achieve rotational speed.

In this chapter a design will be developed for an inertial energy harvester with a centric rotational mass as proof mass. While in literature ample examples of eccentric rotational proof masses can be found, such as in watches, no previous research into harvesters have been found of centric rotational harvester that solely use ground accelerations as input. Also, an extensive research into rotational energy harvesters (Fu et al., 2021) does not mention any examples of inertial rotational vibration energy harvesters.

### 4.3. Effect of main design direction choice on design objective

To achieve rotation of the proof mass, an eccentric force will need to act upon the mass. To allow for forces to act on the mass, there needs to be a difference in velocity between the mass and the body that exerts a force on the mass. Since the only movement in the system is ground movement, the rotational mass or a second body needs to be attached with a spring to achieve relative motion between the ground and the rotational center. In the next paragraph will be discussed what this means for the frequencies under which the harvester should be able to harvest energy.

Having established and analyzed acceleration data that is present in the bridge in the previous chapter, the implications for the rotational energy harvester can be discussed. There inevitably will be some parasitic damping present in the system. To get an initial idea what frequency region the harvester will perform, the system will behave as a simple mass spring damper system. A standard system frequency response of such a system is displayed in Figure 4.3.

The figure consists of two parts. In the upper part the the gain of the amplitude of the mass relative to the excitation frequency versus the excitation frequencies is depicted. In the lower part, the corresponding phase delay is shown. The multiple lines correspond systems with different damping rates ( $\zeta$ ). Two regions are highlighted where a relative motion can be observed between the mass and the ground, a blue and a red region. In both the blue and the red highlighted region, relative movement between the ground and the mass occurs. In the blue region, close to and including the resonance frequency, this is caused by an amplitude gain of the mass compared to the amplitude of the ground accelerations, as can be seen in the top part of the figure, where the amplitude of the mass relative to the input amplitude is shown. In the red region the amplitude of the movement decays quickly, but still relative movement is achieved here due to the phase shift. In the lower part of the figure the phase delay of the mass with respect to the phase of the ground accelerations is displayed. In the red region this phase delay approaches  $180 \text{ deg}$ , which means that the mass moves in the opposite direction of the ground. This means that eigenfrequency from the harvester should be equal or lower than the ambient vibrations in the bridge. As discussed in Chapter 2, all frequencies till around  $50 \text{ Hz}$  can be found in the signal. To be able to harvest most of these frequencies, a low eigenfrequency is preferred. To find how low the the eigenfrequency would preferably be, a fast Fourier transform (FFT) is used to project the acelerations over time from the bridge signal onto the frequency spectrum. This is similar to the spectrogram, Figure 2.2 in Chapter 2, but this one does consider the time aspect. Squaring the values from the FFT and deviding them by the boxwidth, the power spectral density is calculated and the results are shown in Figure 4.4. This figure shows the normalized power per frequency per frequency available in the dataset. As can be observed in the figure, in frequencies from 10 till  $20 \text{ Hz}$  there is a relatively a lot power in the bridge vibrations and, at similar levels, between 30 and  $35 \text{ Hz}$ . As just is determined, the system will the mechanism should be able to harvest energy around or above the eigenfrequency. Combining this finding with the power spectral density plot, the eigenfrequency would

preferably be below 10Hz.

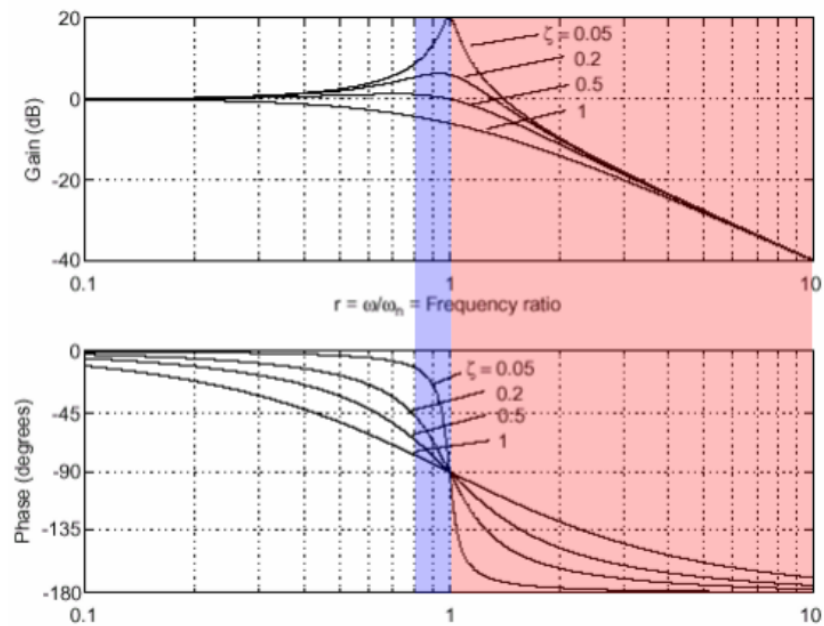


Figure 4.3: Operating frequencies plot. (Based on figure from Phillips and Harbor, 1996)

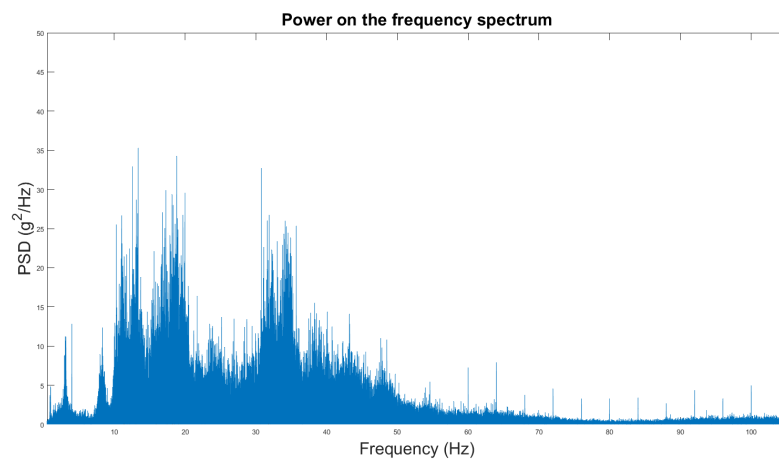


Figure 4.4: Fast Fourier transform of the bridge signal

## 4.4. Sub-functions

In this section the sub-functions found in the harvester are identified. For each of the functions, several solutions will be presented.

- The mass needs to be connected to the ground. Here, different options are available with respect to the orientation of the mass' axis of rotation and the stiffness of the connection of the mass. Considering orientation, a choice can be made between a rotation direction perpendicular to the gravity and a rotation direction in plane with gravity. The axle of the mass can be connected to the ground be solid or with reduced stiffness by using a spring, a damper or combination of the two.

- Movement of the ground needs to be transferred into the mass. An eccentric force acting on the rotational mass can only cause rotation if the body that exerts force on the rotational mass moves respectively to this mass. The stiffness of the attachment of the second body to the ground can not be chosen completely independent of the connection of the mass. To allow relative movement of the mass and the body that exerts a force, at least one of the connections (connection of mass or force transfer body) needs to contain a spring and/or damper.
- Next to creating relative movement, the type of movement needs to be converted. The movement of the ground is primarily linear, in the direction of gravity. This oscillating linear movement has to be converted to a continuous, rotational motion of the mass.
- The energy needs to be harvested from the moving mass and stored. This can be done directly, with a generator. Alternatively, a spring could function as storage for mechanical energy, before it is converted to electrical energy.

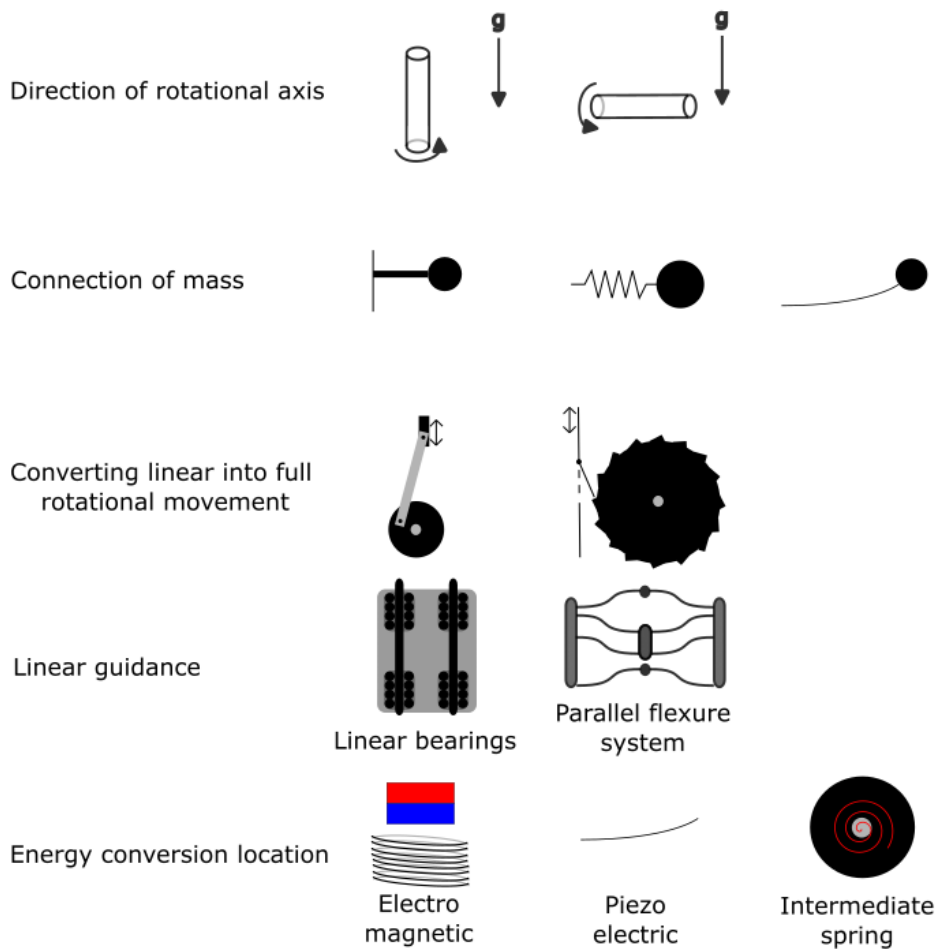


Figure 4.5: Design choices

## 4.5. Choosing sub solutions for the design

### 4.5.1. Orientation of rotational axis

The ground accelerations act predominantly in the direction of gravity. These accelerations are to be converted into rotation of the mass act. In Figure 4.6 both orientations are displayed. In red the force required for the rotation the mass is displayed. As can be seen on the left side of the figure, when choosing a rotational axis in line with gravity, a force (blue in the figure) is needed to change achieve

a force that rotates the mass. Since the ground is moving, it is not trivial how this force is attained. On the right, where the rotational axis is perpendicular to the gravity, this complication does not arise. Therefore, a rotational axis in the horizontal direction is chosen over a rotational axis in the vertical direction or any angle in between.

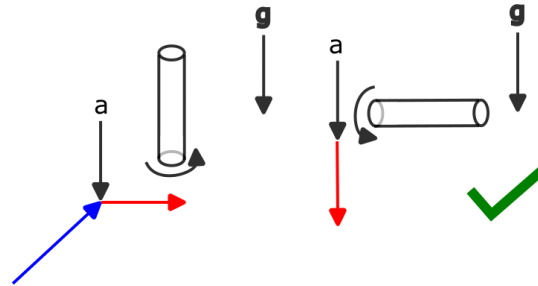


Figure 4.6: Choice in rotational orientation (In black the gravitational direction and ground accelerations, in red direction of force for rotation, in blue the required force for direction change)

#### 4.5.2. linear to rotational

Limited options are available for converting linear to rotational motion, especially when taking into account that the amplitude for the linear movement is not constant and a fully rotational movement is required for the harvester to work as intended. Two general methods are considered for converting linear into rotational movement, displayed in Figure 4.11. The first one is a rigid link, or combination of links, that is eccentrically connected to the mass, with a allowing movement with a rotational point or allowing for sliding. These type of connections only work when the amplitude is constant and movement is continuous, such that momentum of the wheel ensures that the mechanism doesn't get stuck on a dead point (where the eccentric point is in line with the point of rotation and the direction of the force). Also free rotation of the mass, when input accelerations are not present anymore, is not possible with these types of linkages. As movement of the bridge deck does not exhibit a constant amplitude, nor continuous motion and free rotation of the mass, as is required the benefit from the desired advantages of a rotational proof mass, a ratchet type mechanism is chosen to transfer forces from the ground to the wheel. The ratchet mechanism does come with parasitic damping during the free rotation. Another disadvantage from the ratchet mechanism is the engagement angle. This is the angle the mass needs to rotate before engagement with the ratchet occurs, which leads to an interaction force. Especially with the small amplitude of the vibrations, this engagement force requires attention, because the engagement angle could, with small amplitude vibrations take up a large part or all of the amplitude, resulting in little or no rotational movement. All though these disadvantages are significant, no alternative method has been found to convert linear to rotational movement while fulfilling the other requirements. These negative consequences will need to be addressed in other design choices.

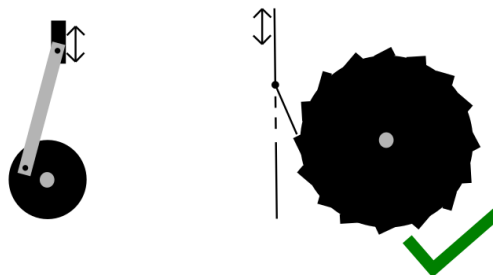


Figure 4.7: Choice for linear to rotational movement

### 4.5.3. Energy conversion location and method

Choosing a specific transducer is out of the the scoop of this research, but a general transduction method has to be chosen because the type of transduction has an effect on the dynamics of the system. Energy harvesters often use either electromagnetic (EM) or piezoelectric (PE) energy conversion. EM transducers perform better under high speeds and PE transducers benefit from high frequency vibrations. Since the accelerations in the bridge are low, the conclusion is that the rotational mass needs to be heavy to attain high interaction forces, speeds found in the takeoff mechanism are expected to be low. Methods exist to increase the rotational speed (for example gears) and an oscillation frequency (frequency up conversion). However, since the bridge vibrations are very irregular, expected is that despite implementation of such techniques, the percentage of transduction time where the transducer will be in a region where it performs efficiently will be limited, when connected directly to the proof mass. For this reason it is proposed to use an intermediate spring to store energy. Chosen is to apply an intermediate spring to harvest energy (Figure 4.9). The rotational spring will store the mechanical energy from the rotation of the proof mass as spring energy (schematically displayed in Figure 4.8). When the spring has stored a certain amount of energy, it engages with a transducer and unwind, allowing the stored spring energy to be converted to electrical energy. With this method the energy storage is displacement dependent since the speed dependent part of the harvester, the transduction is decoupled. The input of the transducer is better controlled because it is not depending on the properties of the traffic, but on the unwinding of the spring. With less variation in the input of the transducer, higher transduction percentages can be reached, considering that the efficiency of EM generators is dependent on the rotational speed and with more control over the input of the generator (**generatorEfficiency**), the optimal rotational speed can be closer approximated compared to a directly coupled generator.

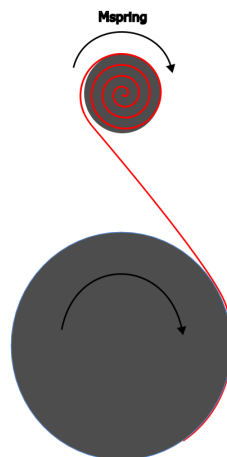


Figure 4.8: Constant moment spring and proofmass

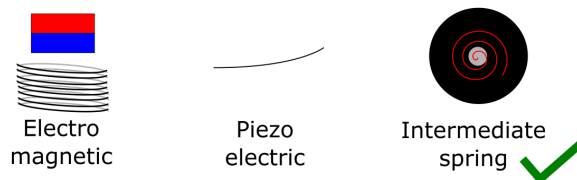


Figure 4.9: Choice for energy conversion

## 4.6. Combining sub solutions into total design

Several solutions have been chosen for the harvester. An overview of the current choices:

- A rotational mass will be used to harvest kinetic energy from bridge vibrations.
- The axis of rotation is perpendicular to the direction of gravity.

- A ratchet will be used to generate an eccentric force on the proof mass.
- Transduction to electric energy will be indirect, using an intermediate spring.

From these principle design choices, two schematic designs have been created (Fig 4.10). These schematic designs will be described and then compared for the intended use situation. After this comparison, a more detailed design will be made, where the spring and guiding of the moving mass(es) will be considered, as well as the ratchet mechanism.

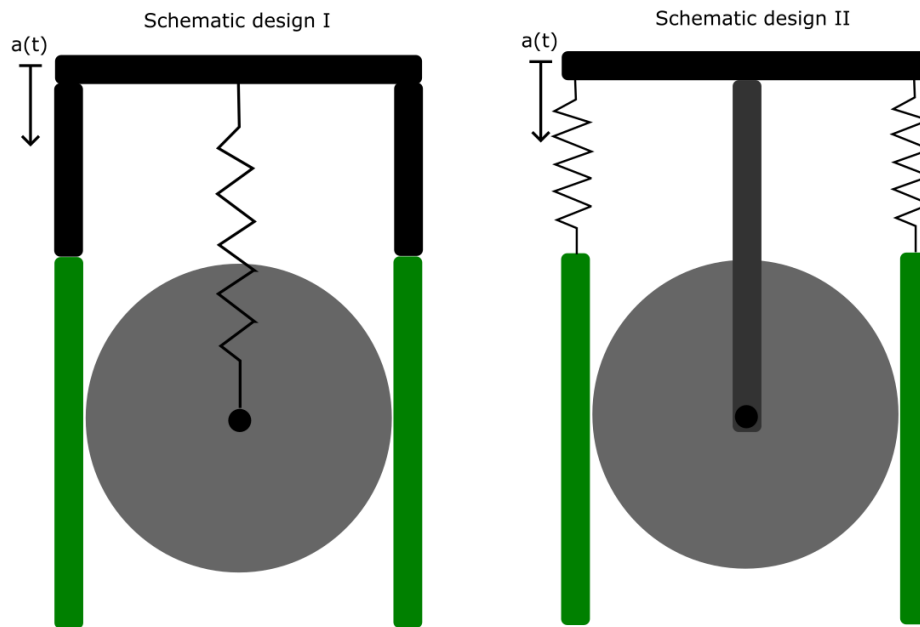


Figure 4.10: Schematic designs of the harvester (in green the ratchets), on the left a design with a translating rotor and on the right a design with translating ratchets

#### 4.6.1. Schematic design I, translating rotor

In the first schematic design, the rotational mass has two degrees of freedom. One translational degree of freedom, in the gravitational direction. The other one is the rotational degree of freedom around the axis at the center of mass, perpendicular to this 2D image. The two linear parts of the ratchet-pawl system are solidly connected to the ground in this design.

#### 4.6.2. Schematic design II, translating ratchets

In the second schematic design, the degrees of freedom are separated. The rotational mass can only rotate, not translate. To allow for relative motion between the linear part of the ratchet-pawl system and the rotational mass, these linear parts are connected with a spring to the ground. They have one translational degree of freedom in the gravitational direction.

### 4.7. Comparison of schematic designs

In this comparison the goal is to choose a design which will have the best expected energy take off performance when excited by the presented bridge excitations. In the translating rotor design, mass is used for in the rotor contributes to the rotational inertia as well as to the linear inertia, while in the translating ratchet design, mass from the rotor only contributes to the rotational inertia and the mass of the ratchets contributes to the linear inertia. As performance wise, both mechanisms would reach similar displacement and rotation when linear and rotational inertia are equal. The translating rotor design uses weight more efficiently and would be able to achieve a lower total weight for the harvester, as the weight of the ratchets would not need to be increased to achieve higher linear inertia. An advantage of dividing the linear and rotational inertia over different masses, is that more flexibility remains in the

relation between the types of inertia. This amount of freedom will only be when necessary very large differences are required in the two types of inertia. At smaller differences, this can be achieved by shaping the rotational mass. As the total weight of the harvester and thus used construction material is considered to be relevant for implementation and there is no inducement yet that ratios between the two types of inertia need to be so large that they are unattainable by solely choosing dimensions of the rotational mass, the translating rotor design is chosen.

## 4.8. Further design choices based on schematic design

With a schematic design for the harvester determined, more specific designs for the spring and linear guiding of the mass the ratchet mechanism will be discussed.

### 4.8.1. Linear suspension and guidance

The moving part is positioned between the two solidly connected parts, the ratchets. In the chosen design, there are a few demands for the connection of the mass. The first one is that the connection needs to allow for translational movement in the direction of gravity. The second one is that the rotational mass needs to stay oriented between the ratchets, meaning no or negligible movement in the plane perpendicular to gravity, and no rotation of the axle of the proof mass.

Two suitable design directions are identified for this design. The first direction are linear guides combined with carriages that run on them. These are low friction due to bearings and are commercially widely available.

The second suitable direction is a set of parallel flexures. These flexures allow movement in the vertical direction. Because they bent instead of roll there should have very little dissipation of energy. Also, the flexures do not require lubrication, in contrary to the bearings in traditional linear guiding systems, which is a advantage for prolonged use in hard to reach places.

If the required translational distance allows for implementation of the flexure design, this would be the preferable solution (Figure 4.11).

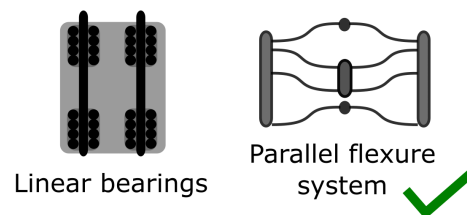


Figure 4.11: Choice in linear suspension and guidance

### 4.8.2. Rectifier

One of the reasons that was chosen for a rotational mass for the power takeoff mechanism, is that energy can be added while the mass by speeding up the rotational speed while it is already moving from previous excitations. For this to work, the force needs to be applied in the direction the mass is moving. This can be done by implementing a mechanism that engages a ratchet such that the interaction force will moved into the current rotation direction. Another possibility is that a rotational direction is chosen for the mass and the ratchets will be installed such that they always exert an interaction force that is in the direction of this chosen rotation direction. Chosen is for a fixed rotational direction because a mechanism for changing interacting direction of the ratchets adds complexity without inducement and requires energy to engage/disengage.

Looking closer into the ratchet, due to the translating rotational center and the intended design idea of being able to add energy into the rotating mass at any point of the translational amplitude, not only in the equilibrium position, a double functionality is required (depicted in Figure 4.12). The first part of this double functionality is the functionality of a linear rack and pinion, which continuously engages a linear rack and a gear wheel over the range of the linear rack. The second is the functionality of an overrunning clutch, which converts the bi-directional rotational movement into a single directional rotational movement.

The double functionality, can also be combined into one mechanism instead of two in series by placing

multiple pawls from a conventional ratchet pawl system in a linear fashion, close to each other. No examples have been found in literature of such mechanisms.

Rectifiers come with some properties that are disadvantageous for this application. An ideal clutch can convert an infinite force in the driving direction and exerts zero moment when the spinning in the free running direction. In practice, there is a parasitic damping moment acting in the free run direction that is caused by moving the parts that are placed to exert force in the driving direction. In the figure that discussed earlier, Figure 4.12, this is mainly caused by the rolling resistance of the balls. Next to the parasitic motion, another disadvantage is found. This is the engagement angle. The engagement angle is the angle that the driving part of the clutch has to rotate in the driving direction before the moving parts are in a position that the driving moment is applied. Again, looking at Figure 4.12, the engagement angle is the angle that needs to be turned before balls are clamped in the between the outer circle and the, with respect to the radian, inclined surfaces on the inner circle.

For the energy harvester, it is important to minimize both of these. The need to minimize parasitic damping reduces energy loss in the system and thus improves energy output. The engagement angle van, especially at relatively small amplitude input vibrations, of great importance. There is a risk of losing a significant part of available energy that enters the system by moving the driving part of the mechanism within the engagement angles, without engaging the proof mass. Part of this risk has been reduced by the choices in transduction. The spring used to store the energy exerts a moment on the rotational proof mass in the opposed to the rotational direction. When the mass comes to a standstill, this moment will turn the mass slightly against the intended rotational direction till it engages. As a result, the mass will always be in the engaged position when the mass is not rotating, allowing to harvest energy shocks and small amplitude excitations. In these cases, the effect of the engagement angle is not observed in a distance that has to be moved before engagement, but rather when the rotating mass comes to a standstill. When a standstill occurs, some energy that is stored in the spring will be lost in the backwards rotation of the proof mass. A smaller engagement angle would mean smaller energy losses at standstill.

When the mass is rotating, the engagement of the mass with the ratchet is not ensured by the negative moment from the harvesting spring. As a result, some of the ground movement that would accelerate the rotation of the mass when using an ideal clutch will not do this in practice. On these effects will be elaborated in Chapter 5.

Choosing a specific ratchet type for the harvester now would be preliminary. An optimal design choice will depend on the forces that are expected in the system. For this, the weight of the proof mass would need to be known, as well as maximum accelerations that are expected to occur in the bridge, also under incidental conditions, to make ensure the ratchet mechanism is able to withstand the forces. Many types of mechanisms can perform the described, required functionality. Choosing a specific one is considered to be part of a later, optimization stage in the design process.

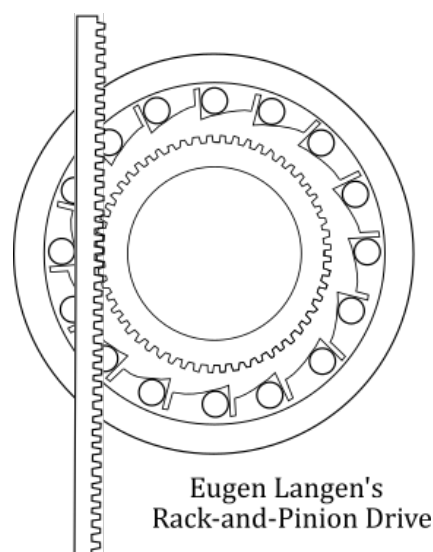


Figure 4.12: Example of transforming linear to rotational motion before rectifying (FrictionPhysics, n.d.)

### 4.8.3. Combining sub-design

Combining all conclusions on sub parts of the system, a final, parametric, design can be made (Figure 4.13). Dynamics and system parameters will be discussed next, in Chapter 5.

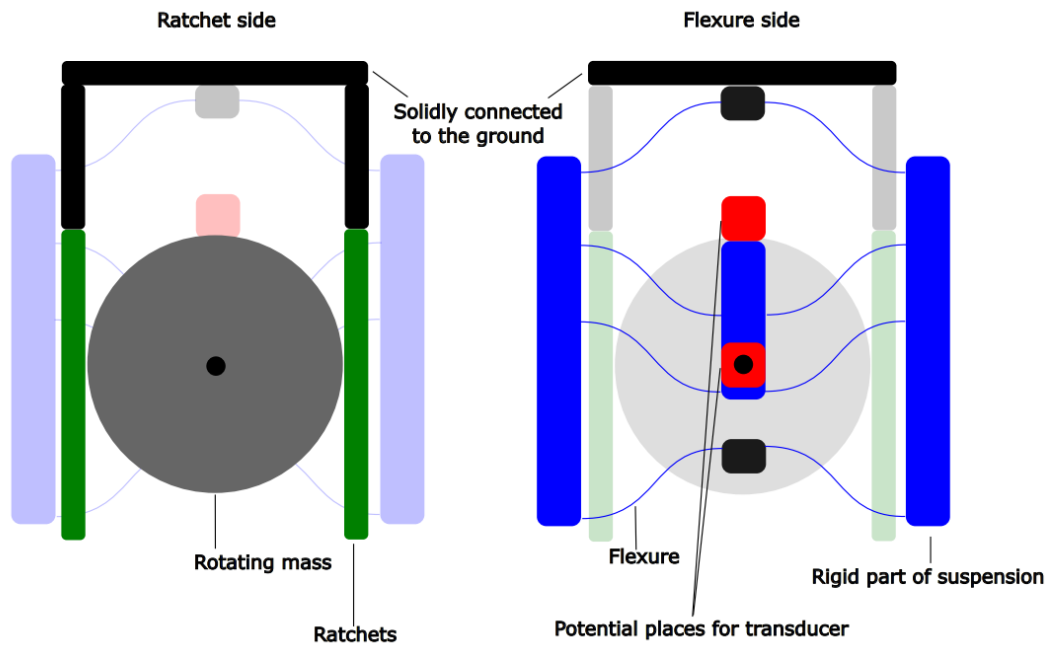


Figure 4.13: Combined choices on sub-designs



# 5

## Model

### 5.1. Dynamics

Having established the basic design of the harvester, the dynamics will be described. For the first order calculations, simplified and ideal components in 2D are used. The system contains two degrees of freedom. The degrees of freedom are chosen as the global location of the center of mass ( $z$ ) and the angle of the mass ( $\phi$ ) (Figure 5.1).

The forces in the system are depending on the inertia of the mechanism and the ground movement. The dynamics of the system will be considered in for two cases, during engagement of the ratchet and without engagement. The criteria for engagement are discussed later in this chapter. Starting with the engaged ratchet, the dynamics of the system can be described by considering the equations of motion in the linear direction (Equation 5.1), and in the rotational direction (5.2).

$$\ddot{z} = -\frac{k_z}{m}z + \frac{\mathbf{F}_r}{m} + \frac{\mathbf{F}_{fric}}{m} + g, \quad (5.1)$$

$$\ddot{\phi} = \frac{r}{I}\mathbf{F}_r - \frac{k_\phi}{I} + \frac{\mathbf{M}_{fric}}{I} \quad (5.2)$$

and, during engagement, the following equation is holds for the ground velocity, and the rotational and translational speed of the proof mass:

$$\mathbf{v}_{ground} = \dot{z} + r\dot{\phi}, \quad (5.3)$$

where:

- $m$  = the suspended proof mass,
- $I$  = the rotational inertia of the proof mass,
- $k_z$  = the spring stiffness in the z-direction,
- $k_\phi$  = the spring moment of the energy storing spring,
- $\mathbf{F}_r$  = the driving ratchet force,
- $\mathbf{F}_{fric}$  = the friction force caused by the ratchets,
- $g$  = the gravitational acceleration.

The system of equations for the engaged can thus be described by three equations (Equations 5.1, 5.2 and 5.3), with three unknowns ( $z$ ,  $\phi$  and  $F_r$ ).

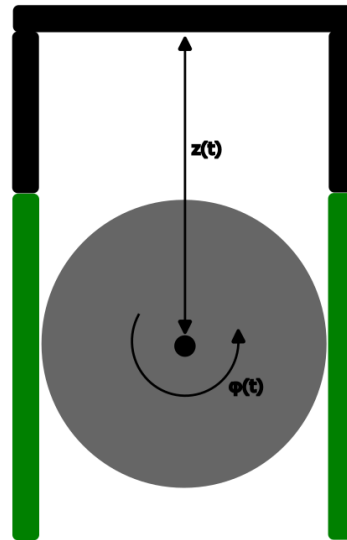


Figure 5.1: Degrees of freedom in the system

As discussed in Section 4.5.3 kinetic energy of the proof mass is, unconventionally, first stored in a spring before being converted. In most vibration energy harvesters, the kinetic energy is harvested from the system with a transducer, which is modelled as a viscous damper to the effect that the stored energy is proportional to the velocity in the system. In this mechanism, the energy is stored in a spring and thus decoupled from the velocity. Therefore it is modeled as a constant moment (with  $k_\phi$ ) in the equation. The friction force in the model is simplified and assumed known and assumed constant, where in reality all sorts of complications arise, such as difference between static and dynamic friction, and changes over time due to changes in surface roughness, interaction surface and lubrication. Another simplification is made for the spring that suspends the proof mass, it is modeled as a spring with a constant spring constant. In the design is chosen for a flexure system to suspend the mass. If the amplitude of the mass vibrations remains small, compared to the flexure length, this simplification can be made. If this ratio becomes larger, this simplification will not hold anymore. For this system and the small amplitude input vibrations with a non-resonant system, the translational amplitudes is expected to stay small, and this simplification can be made.

When there is not ratchet engagement, the system of equations simplifies to the following:

$$\ddot{z} = -\frac{k_z}{m}z + \frac{F_{fric}}{m} + g, \quad (5.4)$$

$$\ddot{\phi} = -\frac{k_\phi}{I} + \frac{M_{fric}}{I}. \quad (5.5)$$

In this second system of equations, the ratchet force is 0, because there is no ratchet engagement. Also, Equation 5.3 does not hold anymore. This reduces the system of equations to a set of two equations with two unknowns. The ratchet force is the driving force of the mechanism and the engagement criteria, magnitude and direction will be discussed next, in Section 5.2.

## 5.2. Force in the system

As the off diagonal quarters of the state space matrix are zero, the two systems are decoupled. The only way they the two systems are related are related is through the interaction force  $F$ . This force acts between the ratchet and the rotating mass. Next to some constant system parameters, the magnitude and direction of the force depend on the rotational and linear speed of the proof mass and on the ground movement. The function of the force is non-smooth, therefore an analytical solution for the equations

will not work and a numerical method is required.

To model this we can use a piecewise function. In Table 5.1, the engagement criteria for different system states is given. In Figure 5.2 a visual representation is given of these criteria. If these criteria are not met, the rotating mass is not accelerated by the ratchet. The engagement angle is not implemented in these equations. Implications of this simplification will be discussed later.

Table 5.1: ratchet engagement criteria

	Ground moving up ( $v_{ground} < 0$ )	Ground moving down ( $v_{ground} \geq 0$ )
Mass moving down	$-v_{ground} > r * \dot{\phi} - \dot{z}$	$v_{ground} > r * \dot{\phi} + \dot{z}$
Mass moving up	$-v_{ground} > r * \dot{\phi} + \dot{z}$	$v_{ground} > r * \dot{\phi} - \dot{z}$

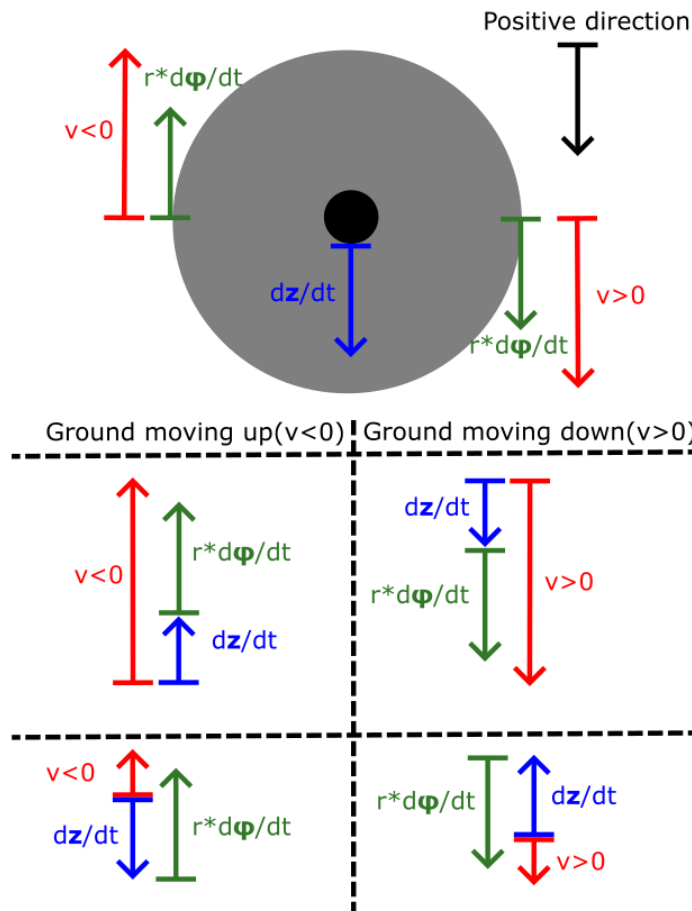


Figure 5.2: Engagement forces

Rewriting the Equations 5.1 and 5.2 for the ratchet force gives the following equations:

$$\mathbf{F}_r = (m + m_{cart})\ddot{z} + k_z z - \mathbf{F}_{fric} - \mathbf{g}(m + m_{cart}), \quad (5.6)$$

$$\mathbf{F}_r = \frac{I}{r} \ddot{\phi} - \frac{k_\phi}{r} + \frac{\mathbf{M}_{fric}}{r}. \quad (5.7)$$

With a given mass, and at the same  $z$  value, the rotational acceleration multiplied with the rotational inertia over the radius is constant. With a higher inertia, a lower rotational acceleration is reached.

While rotation is aimed for, since the rotation will be used to store wind the storage spring, higher rotational speed will lead to less engagement time and with a lower rotational inertia, there is rotational energy in the system at the same velocity is less, and since the rotational speed in the best case is limited by the ground speed and the speed of the mass added (when ground speed opposite to the translational speed of the mass), the inertia should not be too low.

### 5.3. Losses in the system

In harvester, several causes of energy can be found. Losses occur due to parasitic motion and in bearings for the axle of the wheel. The largest expected losses will be caused by the sliding friction of the interaction between the rotation mass and the linear ratchet. This friction force acts in the opposite direction of the rotating direction.

For the modeling of the friction force of three situations are identified:

- Situation 1) No rotational velocity. Without Rotation, there will be no friction.
- Situation 2) Nonzero rotational velocity, no ratchet engagement. In this situation the mass is rotating, while the engagement criteria for ratchet engagement(given in table 5.1) are not met.
- Situation 3) Nonzero rotational velocity, ratchet engagement. In this situation, friction forces occur at only one of the ratchets.

In Table 5.2 conditions and the simplified corresponding friction force and friction moment on the rotational mass are given. In Figure 5.3 a visual representation is presented. When the ratchet is engaged (Situation 3), the friction force force is halved, because in that case sliding occurs at only one of the the ratchets. Value for the friction force will depend on the type of ratchet, specific dimensions of the wheel in interacts with and the used material.

Table 5.2: Friction forces

Situation	$\Sigma \mathbf{F}_{fric}$	$\Sigma \mathbf{M}_{fric}$
1) $\dot{\phi} = 0$	0	0
2) $\dot{\phi} > 0, \mathbf{F} = 0$	$-\mathbf{F}_{fric} + \mathbf{F}_{fric} = 0$	$\mathbf{M}_{fric} = -2 * r *  \mathbf{F}_{fric} $
3) $\dot{\phi} > 0, \mathbf{F} > 0$	$\mathbf{F}_{fric} = \text{constant in the direction of } \mathbf{F}$	$\mathbf{M}_{fric} = -r *  \mathbf{F}_{fric} $

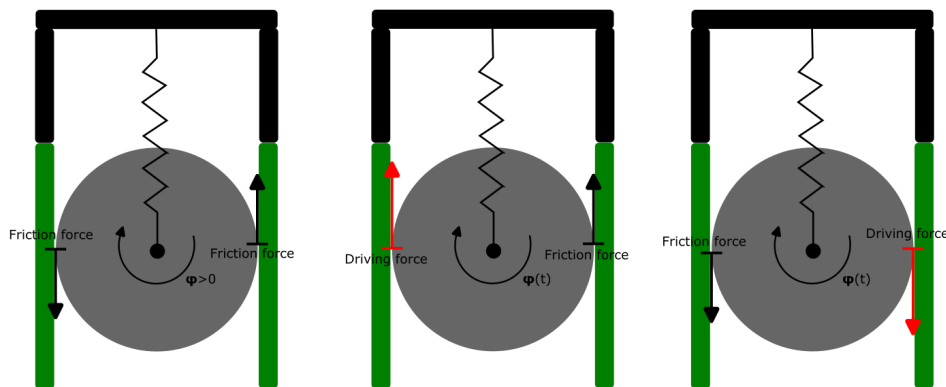


Figure 5.3: Friction force during free rotation (left in the figure) and friction force during ratchet engagement for both the left ratchet (in the middle of the figure) and right ratchet (right in the figure)

Expected is that some viscous damping will be present in the system in the bearings. As the speeds are expected to be low and the spring force that harvests energy from the system is expected to dominate the kinetic energy decline of the system, viscous damping is disregarded.

# 6

## Model analysis

This model will be used to obtain insight in whether the mechanism will be able to harvest energy, and if so, what the order of magnitude the system parameters should be. Simplifications in the model need to be taken into account when interpreting the results from the model. Two important effects need to be taken into account. One is the absence of the engagement angle in the model. When the wheel is accelerated during while it is already rotating, in reality (a part of) the ground oscillation will take place without engagement. This will lead to an overestimation of the interaction force. The second simplification one needs to be taken into account when the rotated or translated distances between moments of zero rotational speeds are very low. In this case, the mass ratchet will not reach the next tooth of the ratchet and the harvested energy is lost when the harvesting moment pushes the proof mass back to initial interlocked position. This simplification leads to an overestimation of harvested energy.

The system of equations, presented in Chapter 5 is programmed in MATLAB. Due to the piecewise nature of the ratchet force, an analytic solver will not suffice for solving the set, therefore a numerical is used to solve the presented set of differential equations with a part of the bridge vibrations as input vibrations and find the values of the general coordinates and their derivatives over time. The used solver is the *ode45* function from MATLAB.

Stored energy is estimated by multiplying the angular displacement by the harvesting moment. To reduce the order of variables, The proof mass will be modeled as a solid, steel cylinder. This means that rotational inertia, linear inertia and weight of the rotational mass are determined by the diameter and thickness of the mass.

In this chapter, the a short part of the bridge accelerations presented in Chapter 2 has been taken as a test input for the simulations, specifically, an 8 second interval from 995s till 1003s from the dataset. This interval has been chosen because there are multiple envelopes with in this relatively short interval that are considered representative in terms of acceleration envelopes (i.e. do not contain values that are considered outliers, reached acceleration values are found in many envelopes of increased acceleration). A relatively short (compared to the length of the dataset) is chosen because took significant amount of time and as simplifications are made, the optimized values for system parameter from the simplified model output expected to differ from real life optimal parameters. The model is used to determine the order of magnitude of the system parameters and observe sensitivity towards parameter changes. With this acceleration profile as input, stored energy has been calculated during simulation for several values of one system parameter while keeping the other values constant. Findings of these simulations are presented in the next few paragraphs.

### 6.1. Mass

Simulation have started with the weight of the rotational proof mass. Remaining system parameters have been set at the constant values.  $k$ , the stiffness of the spring in the  $z$ -direction is set at  $1000N/m$ . Friction force is set at  $0.05N$ . Radius of the mass is set at  $0.05m$ . The harvesting moment is set at  $0.01Nm$ . The density is set at  $7800kg/m^3$ , the density of steel. The mass is changed by increasing

the thickness of mass. As the rotational inertia (of a solid disk) as well as the translational inertia scale proportional to the mass, the ratio stays constant. From the numerical solver of the model presented in the previous chapter(5), a higher mass leads to higher stored energy, as can be observed in 6.1, where the magnitude of the mass is on the  $x$ -axis and the stored energy on the  $y$ -axis. This observation is in line with expectations because the force that accelerates the proof mass is caused by the inertia of the mass and the largest losses, the ones from the ratchets, are independent of the weight.

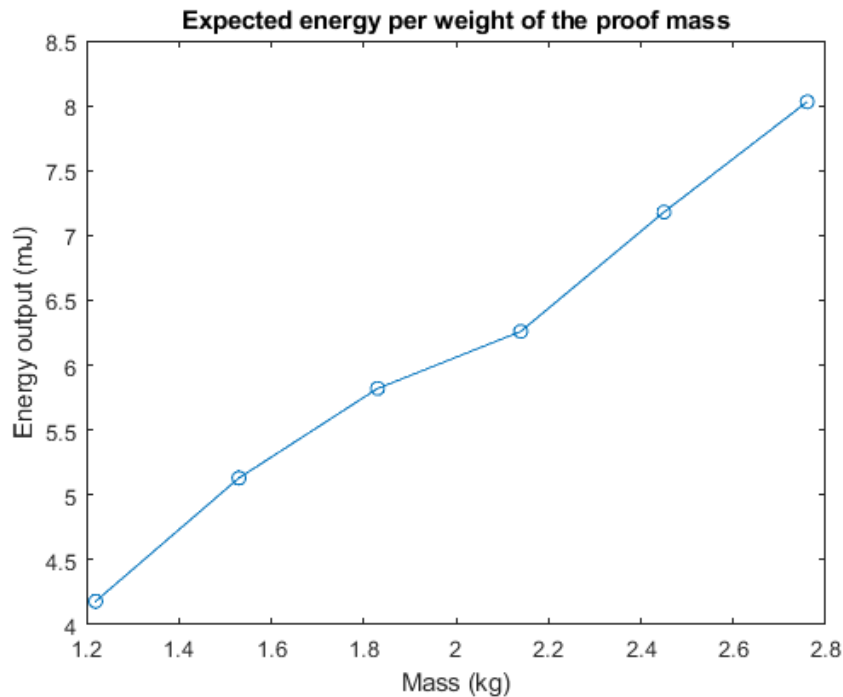


Figure 6.1: Simulated energy output with varying mass

## 6.2. Spring stiffness

For the simulation of the spring stiffness, most values for the system parameters have been used as in the previously mentioned. For the thickness of the mass, three values have been used 20, 30 and 40mm, resulting three values for the mass 1.22kg, 1.83 and 2.45kg to see if whether the sensitivity varies at different values for the mass. The stiffness of the spring, now varies and is set on the  $x$ -axis in Figure 6.2, the stored energy is set on the  $y$ -axis. Important when interpreting the values from Figure 6.2 is that the model uses an ideal ratchet. Due to this simplification, the model will convert all translational movement into rotation, independent of the amplitude of the translation. In practice, this is not the case. Small amplitude translations will not lead to energy storage because the next tooth of the ratchet is not reached, which is further elaborated upon in Chapter 7. Looking at the Figure 6.2, the highest performance is expected at very low stiffness, in the figure the highest simulated stored energy can be found at a stiffness of 10N/m, at higher stiffness (100N/m), the energy has declined a lot. Increasing the stiffness further, at the lowest two weights a small increase is observed. At the higher weight, this increase is larger. Taking this into account the just mentioned simplification, expected is that this ratchet effect plays a larger (negative) role at higher stiffness. This is expected because at higher stiffness, amplitudes are smaller at similar force. In the model, small amplitude vibrations are converted into rotation, but in real life, with small amplitude vibrations, the next tooth of the ratchet is not reached and the energy from these vibrations is thus not stored.

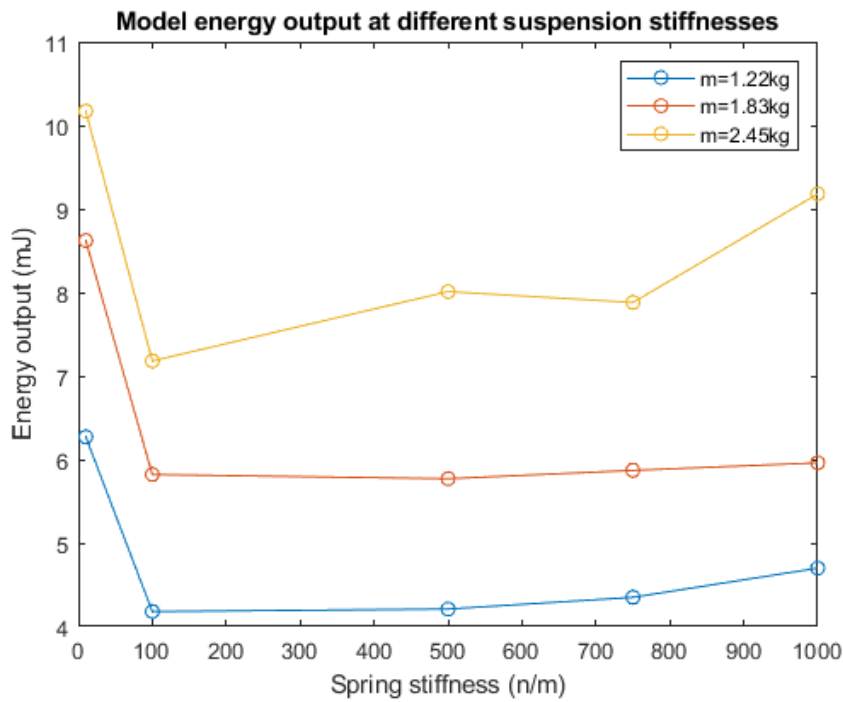


Figure 6.2: Simulated energy output with varying spring stiffness

### 6.3. Radius of force

For the analysis of the effect of the radius of the ratchets on the energy storage, the same values for the system parameters are used. Again the analysis is done for three values for the weight of the proof mass. The stiffness is set at  $100\text{N/m}$  during the simulations. From the result of the model, a smaller engagement radius when Figure 6.3. With a larger mass this effect increases. This is in line with expectations if theory is followed. When the same acceleration is applied at a shorter distance from the rotational point, a higher rotational speed is achieved because:

$$a = r\ddot{\phi}. \quad (6.1)$$

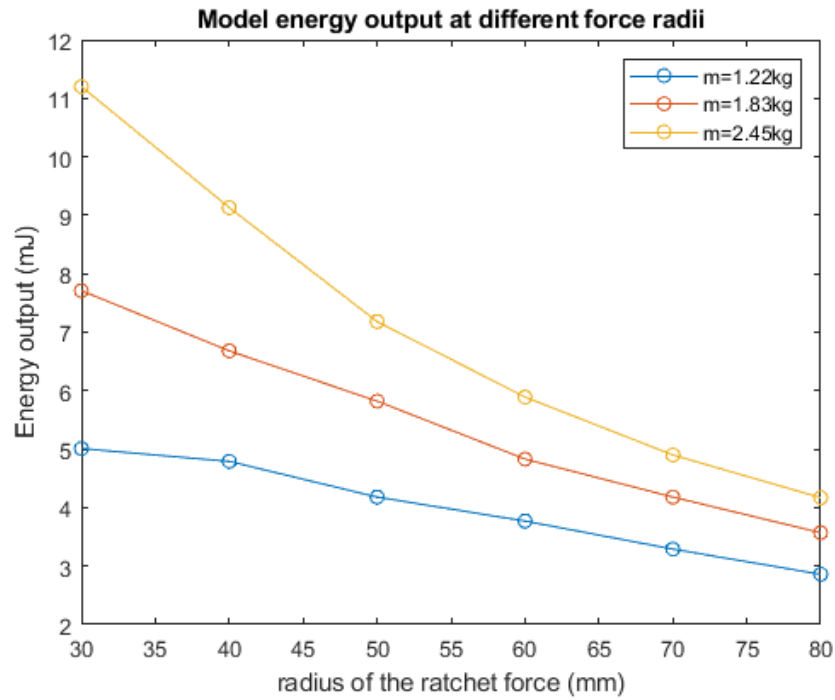


Figure 6.3: Simulated energy output with varying radius of the ratchet force

## 6.4. Harvesting moment

From Figure 6.4 can be observed that for these low amplitude, low frequency vibrations, smaller harvesting moment reach higher simulated stored energy outputs. Larger moments seem to hinder the rotation of the mass too much.

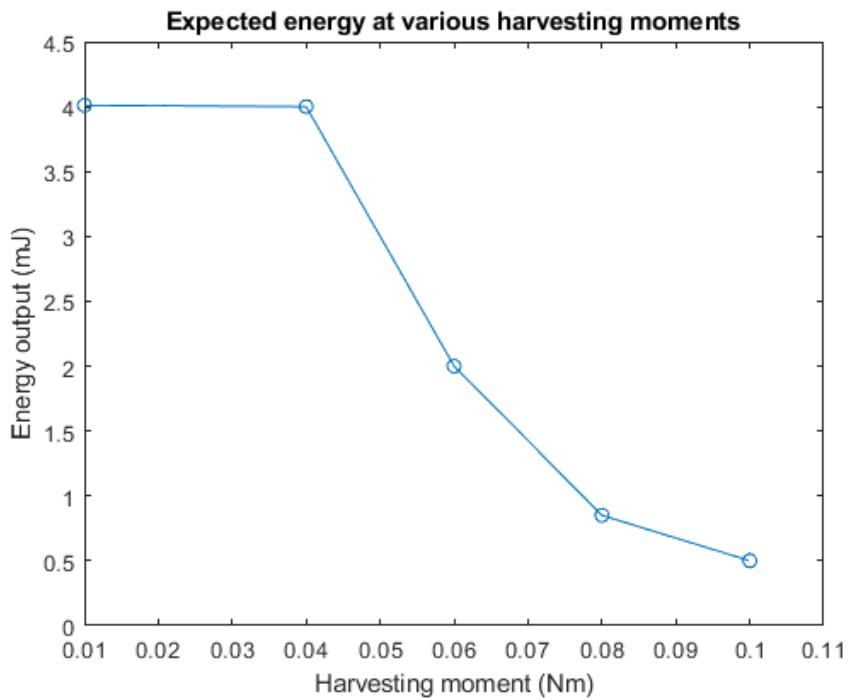


Figure 6.4: Simulated energy output with varying harvesting moment

---

Implications from the findings of this chapter for the proof of concept will be discussed in the next, in Chapter 7.



# 7

## Proof of concept

The purpose of the proof of concept is to examine whether the designed harvester works as expected. To acquire insight in the performance of the design in practice, a simplified version of the design with similar system properties to design presented in Chapter 4 will be build. This mechanism will be tested under various excitations, which will be discussed further in Chapter 8.

In this early development stage of the design, with no similar harvester found in literature, the focus will be on low cost, low production time and simplicity in manufacturing and assembly of the individual parts and the total harvester while still fulfilling the minimal required functions in the mechanism to perform.

### 7.1. Parameter choices

#### 7.1.1. Rotational mass

Decided is to start with the proof mass and base the choices of the other parts on the properties of the mass. There are some contradictory aspects that need to be taken into account. From the model and theory follow that a larger mass would lead to higher interaction force and larger operating frequency range (with constant stiffness). From a cost and handleability perspective, a lighter mass would be more beneficial. In addition to that, other parts will need to be able to withstand higher interaction and gravity forces. At last, limitations of the shaker will need to be taken into account. Aimed is to limit the total weight of the mechanism below  $5kg$ . For the rotational proof mass, a solid steel disc is chosen with a radius of  $10mm$ . The type of steel is  $S235$ . with a density of  $7800 \frac{kg}{m^3}$ , the weight is approximately  $1.82kg$ . Combined with the other parts of the mechanism, which will be mentioned hereafter, the total weight of the mechanism is just over  $4kg$ , remaining within the estimated boundary for shaker.

#### 7.1.2. Frame

Parts of the mechanism will need to be oriented with respect to each other. The mechanism will need to be attached to the shaker. To maintain versatility during the production process and have a lightweight construction with enough stiffness and strength to endure testing a frame will be used. This will be constructed with a standard, aluminum 2020 construction profile with V-groves to facilitate the attachment of parts. Chosen is for a frame with two pillars, such that the mass can be placed between the two, to limit eccentric loading of the guidance system, which could lead to additional friction. With the beam on top, higher stiffness is created in the frame and it allows for the attachment of a spring in line with the center of the proof mass.

#### 7.1.3. Linear guidance and spring

In the design presented in Chapter 4 is chosen for parallel flexures to keep the mass centered and reach the required stiffness of the suspension of the proof mass. Requirements and goals for the proof of concept differ from the eventual harvester that is to be implemented. The proof of concept is will not operate for longer stretches of time in a standalone manner. A flexure mechanism would need to be designed specifically for this mechanism, while advantages for short term use are limited. To reduce

production time and costs, off the shelf products will be used for the linear guidance and suspension. For the linear guidance, two rails and two carousels will be attached to the frame. Parts to attach the connect the axle of the rotational mass to the carousels will be laser cut from PLA.

For the suspension, a spring will be used. As concluded in the previous chapter, a low stiffness is preferred, but the spring needs to be able to deform enough to carry the proof mass and allow for oscillations in the gravitational direction. In addition to possible failure of the spring, the minimal frame height is also dependent on the initial spring length and spring deformations. To fulfill the requirements, a compression spring is selected with a stiffness of  $100 \frac{N}{m}$ , an initial length of  $100mm$  and an outer diameter of  $10mm$ .

#### 7.1.4. Rectifier ratchet

The requirements of the ratchet have been elaborately described in section 4.8.2. An integrated combination a clutch and a rack and pinion system has not been found in off the shelf products and would need to be combined from several off the shelf products. For this proof of concept, an attempt is made to produce part that integrates both these functions while still maintaining sufficient functionality. This will lead to larger tolerances and losses in the mechanism, but since the aim of the mechanism is to see under what sort of excitations such type of harvesters would perform and quantity of the harvested energy is not of the main objective.

Many, close together placed pawls in combination wheel with teeth connected to the mass has been mentioned as a possible design solution for this application. With rapid production methods such as 3D printing or laser cutting of plastics limit the minimal dimensions of small part. Since no designs for these type of ratchets have been found, the decision was made to produce a simpler solution (schematic design in figure 7.1). A rack with a sawtooth pattern is combined with a sawtooth type of rotor with teeth in the reversed direction such that the faces with the steep angles interact with each other in the driving direction to ensure engagement and the faces with the shallow angle interact the when the wheel is spinning without engagement, to reduce the friction force.

The rack will be produced with from a lightweight material and connected with flexures, such that the rack as whole will move from between an engaged and disengaged orientation. This way there is no need for small parts and the distance between consecutive engagements can be limited. This type of ratchet has a disadvantage that losses are higher because the whole rack will need to be pushed out of the way by the rotation of the mass, leading to higher losses. However, the mechanism is expected to perform well enough to serve the goal of the tests while limiting production time and costs.

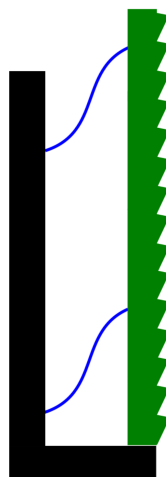


Figure 7.1: Simple ratchet mechanism (in black the ground in green the ratchet profile, in blue the flexures)

## 7.2. Ratchet wheel

For the ratchet wheel, the diameter and the teeth size can be chosen. The ratchet wheel diameter was based on a parameter search performed with the model Chapter 5 With the chosen values for the mass

and stiffness, and a assumed value for the friction force of  $0.05N$ , and other values constant and as input a part of the bridge acceleration data. The friction force was not known, but changes within the order of magnitude did not lead to another outcome for the wheel diameter.

As the minimal engagement angle is dependent on the size of teeth of the engagement wheel and the minimal tooth size is assumed to be constant(if anything, the teeth at smaller diameter would need to be larger due to larger force), a larger wheel diameter would lead to a smaller engagement angle. Due to an error in an earlier version of the model was found that, the sensitivity was found to be very low. Based on these findings, combined with the just before mentioned impact of the teeth size on the engagement angle, a ratchet wheel with a diameter of  $100mm$  is chosen. Based on Figure 6.3, that was found after building and testing, a smaller radius wheel would have been chosen For the shape of the size of the teeth, an angle of  $6^\circ$  is used.

**Harvesting energy** Due to the same error in an earlier version of the model was found that, with previously mentioned parameter values, under bridge excitations, maximum energy is stored when using a harvesting movement of  $0.05Nm$ . To achieve this moment, a constant force spring of  $1N$  is attached to the mass with a radius of  $0.05m$ . Based on the findings from 6.3, a smaller harvesting moment would have been used for the bridge vibration tests.

For the harmonic excitations, since they contain a lot more energy and the off the shelf springs have limited operating length, a constant force spring with a force of  $1.92N$  will be used. The spring will be wound up around the rotation mass. For the test, the spring displacement will be used to estimate the stored energy.

### 7.3. Total mechanism

Combining these design choices into a mechanism has lead to to the result for the proof of concept that is displayed in Figures 7.2, 7.3, 7.4 and 7.5

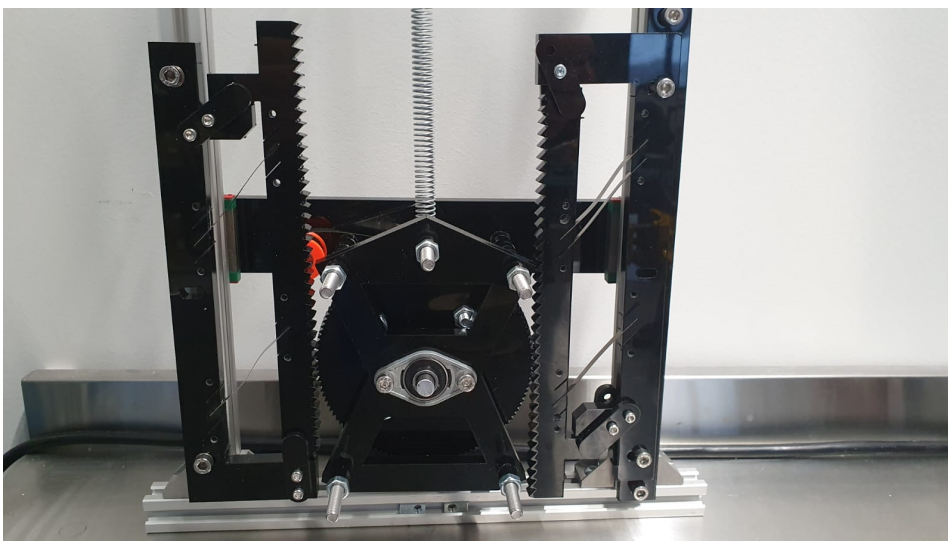


Figure 7.2: Proof of concept picture 1

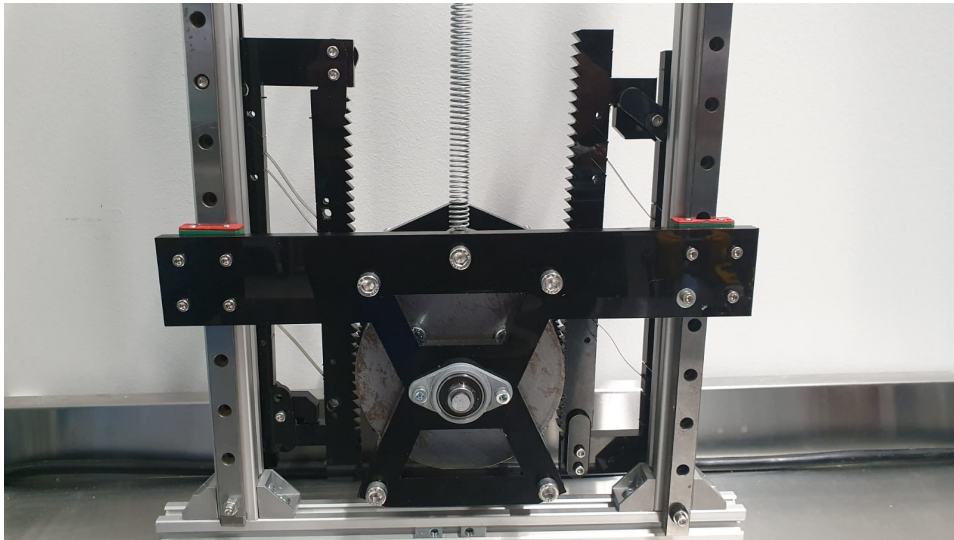


Figure 7.3: Proof of concept picture 2

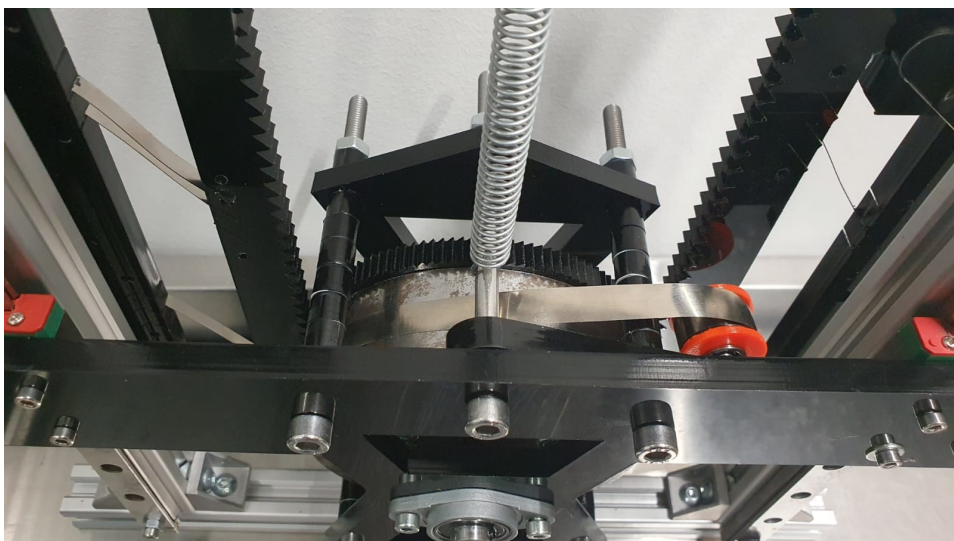


Figure 7.4: Proof of concept picture 3

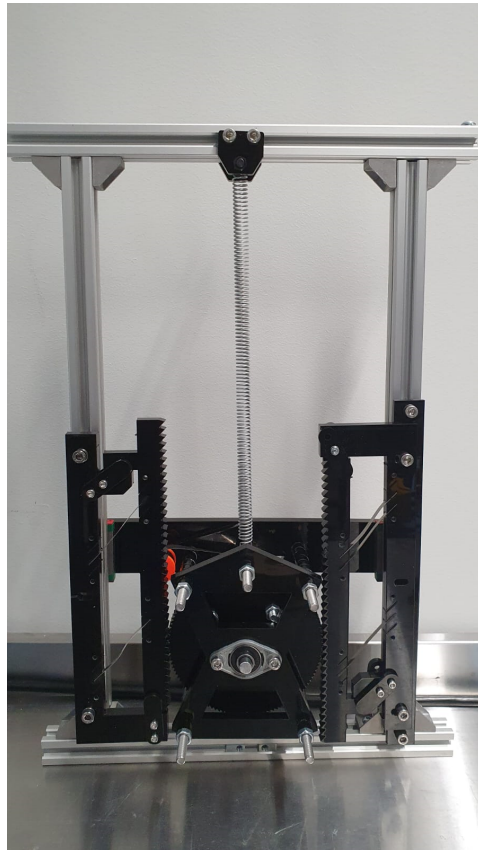
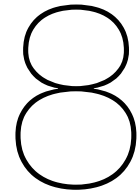


Figure 7.5: Proof of concept picture 4





# Tests and Results

## 8.1. Goal of testing

The goal of the test is to establish under what kind of excitations the system is able to harvest energy. The harvester is in early stages of design, so the main objective of the tests will be observing the behaviour of the harvester. Stored spring energy will be given, but this will not be converted to electrical energy in this research.

The tests will be performed on a shaker (shaker type: Bruel & Kjaer, model:V555, M6-CE). For comparison and repeatability of tests, the harvester will be subjected to some general type excitations. After general excitations, more specific bridge excitations will be implemented. With the tests, limitations of the shaker need to be taken into account. The total weight of the prototype is approximately  $4kg$ . The tests will be divided into three parts: harmonic excitations, shock excitations and bridge specific excitations. In this chapter, the input signals will be presented, followed by the test results.

## 8.2. Harmonic excitations

### 8.2.1. input signal for harmonic excitations

Sine wave functions with multiple frequencies will be used to establish an insight in which frequency range the mechanism is able to harvest energy. For each frequency, a range of amplitudes will be used. This will provide information on a minimum required amplitude of vibration, and possible changes in this minimum under different frequencies.

The test is performed in the following way: The blue results in the plot from tests with a total duration of  $10s$ . The shaker used a ramp up time of  $3s$  before reaching the eventual the amplitude given on the  $x$ -axis of the plots. During the initial three seconds, the amplitude inclines exponentially, before reaching the test amplitude. The input of the  $10Hz$  harmonic tests with normalized amplitude have been plotted in Figure 8.1. The  $15Hz$  and  $20Hz$  tests follow the same amplitude profile with respect to time.

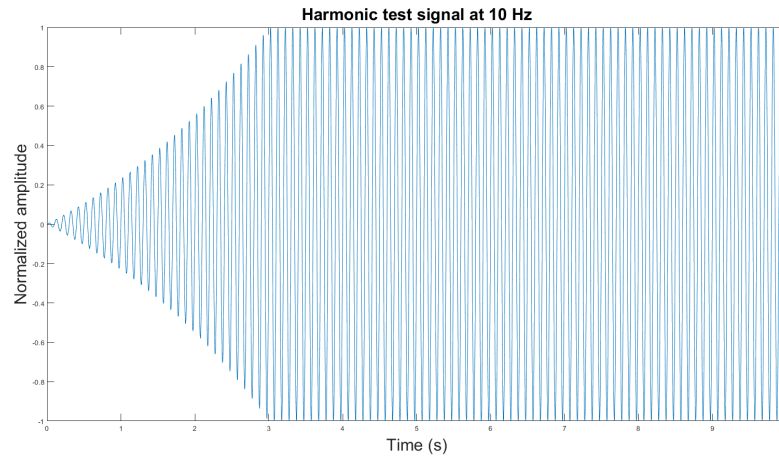


Figure 8.1: Input for 10Hz harmonic tests with normalized amplitude

### 8.2.2. Results from harmonic tests

In Figure 8.2, Figure 8.3 and Figure 8.4 stored power from a harmonic, sinusoidal input are displayed for 10Hz, 15Hz and 20Hz respectively. The green and yellow results in the plots have been measured in a shorter time interval due to the maximum performance region of the constant force spring that was used. The green results have a total test time of 7 seconds with a 3 second build up of amplitude. The yellow results have a total test time of 5 seconds, again with a build up time of 3 seconds. These short periods leave a relative short period on the test amplitude. This has some implications for interpretations of the results, as will be discussed in 8.2.3. The stored energy is calculated by measuring the angular displacement of the mechanism after the described input acceleration. This angular displacement converted to the distance the spring is pulled out. This distance is divided by the total time of the test before it is multiplied by the force:

$$\text{Stored power} = \frac{\Delta\phi(2 * r_{mass}k_{spring})}{t_{total}} \quad (8.1)$$

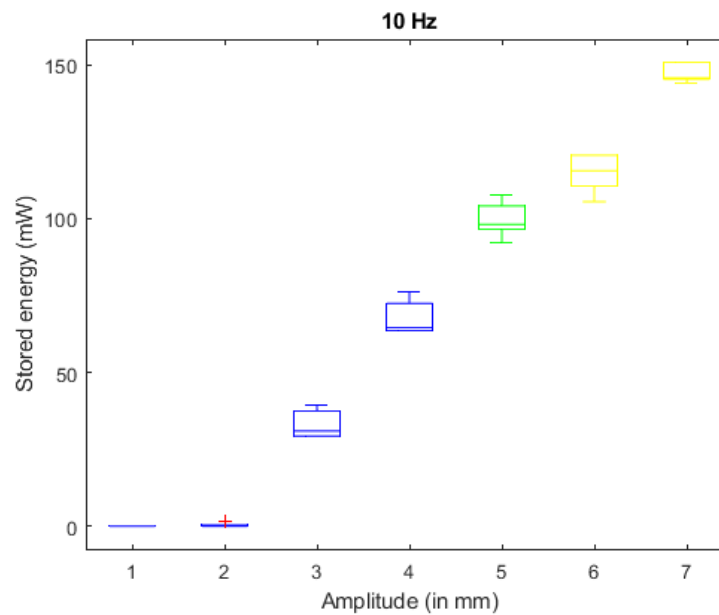


Figure 8.2: Boxplot 10Hz excitations

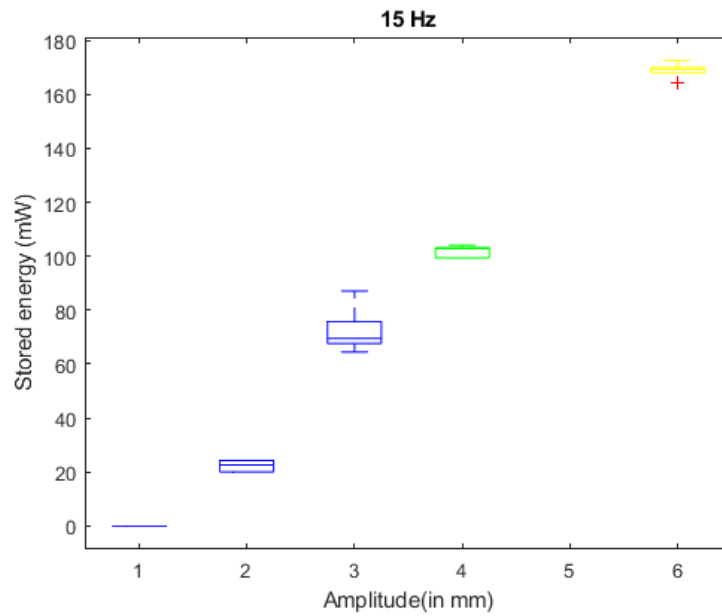


Figure 8.3: Boxplot 15Hz excitations

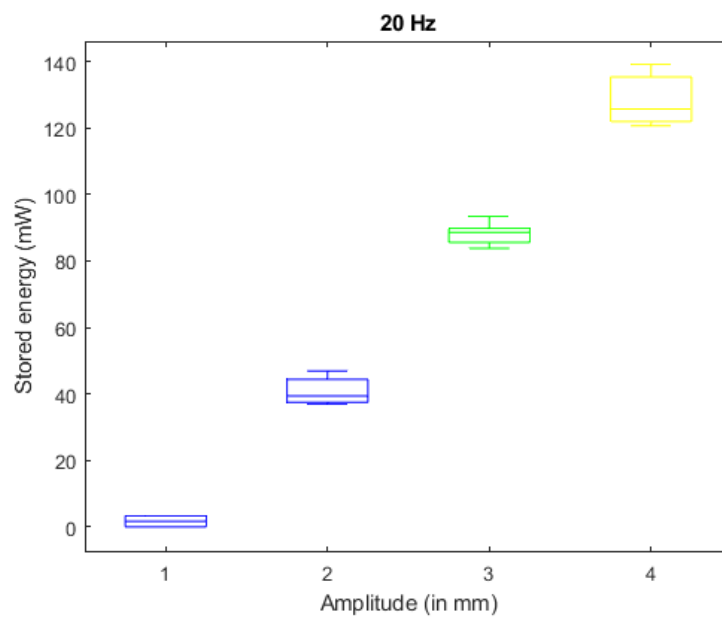


Figure 8.4: Boxplot 20Hz excitations

### 8.2.3. Result interpretation

The mechanism is able to harvest energy from accelerations starting of  $0.6g$ , at  $10Hz$ , at this frequency and acceleration, the amplitude is  $3mm$ . As expected, for higher frequencies and higher amplitudes, the harvester is also able to store energy. At higher frequencies, the mechanism also stores energy at lower amplitudes.

Comparing the amplitudes and frequencies from the harmonic excitations to the measurements from the bridge, peaks in the measurements, similarities can be observed with the  $10Hz$  and  $2mm$  harmonics. Both have maximum accelerations around  $4m/s^2$  and corresponding displacements in the dataset are between  $2$  and  $3mm$ . During the test was observed that the mass turned a little, but not enough

Frequency (Hz)	Amplitude (mm)	Test time(s)	Stored E (mJ)
10	1	10	0
	2	10	3
	3	10	332
	4	10	679
	5	7	699
	6	5	575
	7	5	737
15	1	10	0
	2	10	223
	3	10	724
	4	7	712
	6	5	844
20	1	10	17
	2	10	409
	3	7	617
	4	5	642

Table 8.1: Stored energy in harmonic tests.

Accelerations	1mm	2mm	3mm	4mm	5mm	6mm	7mm
10Hz	.2g	0.4g	0.6g	0.8g	1g	1.2g	1.4g
15Hz	0.45g	0.9g	1.4g	1.8g		2.7g	
20Hz	0.8g	1.6g	2.4	3.2			

Table 8.2: Maximum accelerations during harmonic vibrations

to reach the next tooth. This leads to the expectation that the harvester will not perform with setup in under bridge excitations. In an attempt to improve performance, a ratchet wheel with smaller teeth is produced. These smaller teeth lead to a smaller engagement angle, which is expected to lead to better performance under small accelerations. The angle per tooth is reduced from  $6^\circ$  to  $3^\circ$ .

#### 8.2.4. Improved ratchet wheel performance

The improved ratchet wheel with smaller engagement angle does, as expected, perform better at low accelerations and small amplitude vibrations. This can be observed in 8.5. A large improvement is shown in the harmonic excitations that have been identified to show the similarities with the peaks in the bridge acceleration data.

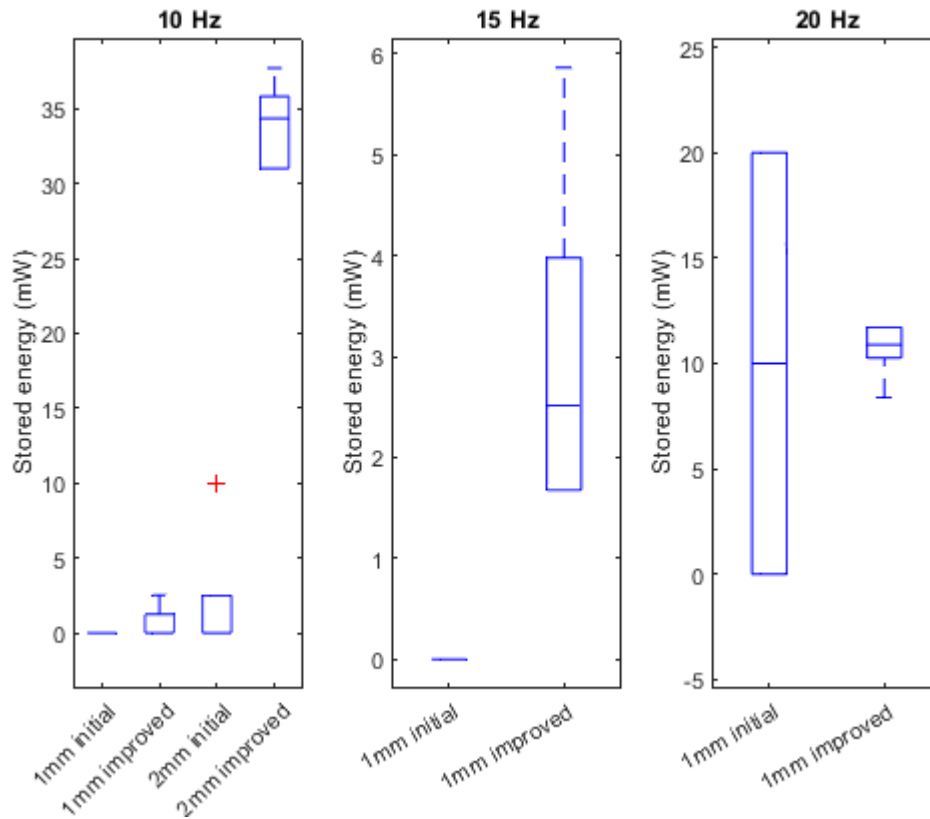


Figure 8.5: Harvester performance with improved ratchet wheel

### 8.3. Shock excitations

The second type of excitations are shocks. This harvester is specifically designed to be able to harvest energy from shocks and non-harmonic excitations. Chosen for shocks is to evaluate performance for non-harmonic excitations because it is an often used non-harmonic excitation. The test will use accelerations in the same order of the bridge accelerations. This proof of concept was built for such excitations, much higher accelerations might require different system parameters and material choices. For the shock tests, variations will be made in duration and maximum acceleration of the shock. Often used input shapes for shocks are half sine, trapezoid and block. Chosen is for the half sine, this one seems most commonly used (among others for military standard testing) and can be performed with less advance machines. The acceleration value and shock duration can be found in Table 8.3. The duration of the shocks have been chosen correspond to the more dominantly available frequencies in the system, that have been identified in Chapter 2 (10, 15, 20, 30 and 40Hz). In Figure 8.6, a normalized shock input is displayed. For the tests, the improved ratchet wheel with an engagement angle of  $3^\circ$  is used.

#### 8.3.1. results from shock tests

In Table 8.3, the energy stored as spring energy is presented. The presented numbers are an average from ten shocks. The lower two cells in the column of shocks with a duration of 50Hz are empty because the displacement amplitude of the shock exceeds the shaker limits. The corresponding amplitudes in mm are displayed in Table 8.4.

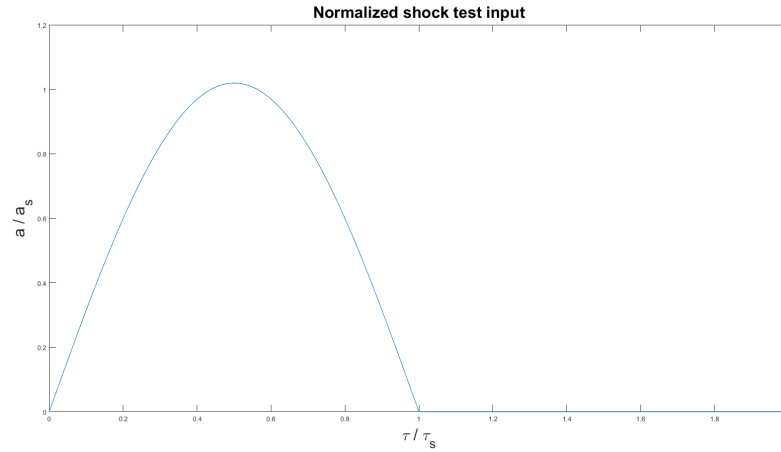


Figure 8.6: Normalized input for shock tests. On the  $x$ -axis is the normalized time displayed, with  $\tau_s$  the shock duration. On the  $y$ -axis, the normalized acceleration is given, where  $a_s$  is the test amplitude.

Duration(ms)	50	33	25	17	12.5
Accelerations					
0.4g	6.3mJ	3.1mJ	0mJ	0mJ	0mJ
0.6g	11.7mJ	5.4mJ	3.1mJ	0mJ	0mJ
0.8g	20.7mJ	5.8mJ	5.8mJ	2.7mJ	0mJ
1g	31.9mJ	12.3mJ	8.1mJ	3.6mJ	0mJ
1.5g	-	28.8mJ	14.4mJ	8.1mJ	0mJ
2g	-	45.8mJ	26.1mJ	9.4mJ	3.6mJ

Table 8.3: Energy stored during shock excitations

Duration (ms)	50	33	25	17	12.5
Accelerations					
0.4g	6.2mm	2.7mm	1.5mm	0.7mm	.4mm
0.6g	9.4mm	4.1mm	2.3mm	1.1mm	.7mm
0.8g	12.5mm	5.5mm	3.1mm	1.4mm	.9mm
1g	15.6mm	6.9mm	3.9mm	1.7mm	1.1mm
1.5g	-	10.3mm	5.9mm	2.7mm	1.7mm
2g	-	13.8mm	7.8mm	3.5mm	2.2mm

Table 8.4: Amplitudes from shock excitations

### 8.3.2. Shock input result interpretation

From the results it is clearly visible that the harvester is able to extract energy from ambient shocks. Larger amplitude excitation under the same shock duration excitations lead to higher stored energy. Except for the last column, in general can be observed that under similar amplitude, with higher acceleration, a higher energy storage is reached.

## 8.4. Bridge specific excitations

Next to performance in general and repeatable harmonic and non-harmonic tests, expected performance for the intended use situation will be tested for. This will be done in two ways. The first way is by identifying a mathematical signal that resembles the measured excitations and subjecting the harvester to this signal. Results from this test will allow for comparison with harvesters for this specific application or applications that resemble it. The second step is subjecting the harvester to the excitations from the measurements.

For the mathematical signal that resembles the input acceleration, an resemblance between the the measured excitation and a sine function multiplied by an envelope is found. An example of such a signal is given in Figure 8.7. The height and width of the Gaussian envelope can be altered to fit the measured accelerations. The shape of the envelope in the signal differs throughout the signal. Some have a longer build up and decay in the amplitude than others, some have a (few) very high peaks in the middle of the envelope, where others are shaped more smoothly. An envelope with a peak of  $4m/s^2$  and a width of 2 seconds is chosen based on visual inspection of the acceleration data. To mimic the wide range of frequencies that can be found in the bridge data, sinus waves with 5 frequencies will be used within the envelope, compared to only one in the example image.

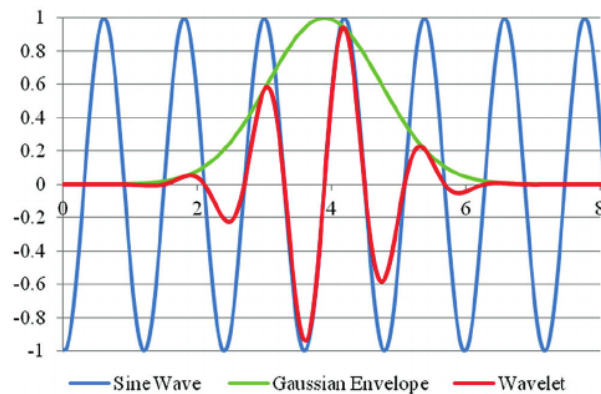


Figure 8.7: Example of Gaussian envelope multiplied by sine function (Mosey et al., 2013)

## 8.5. Bridge specific excitations

### 8.5.1. Gaussian envelope

The signal used for the test is displayed in Figure 8.8 and comprises of sine wave functions with frequencies of 5, 11, 17 29 and 90Hz. This frequencies were chosen by combining the spectrogram and by visually comparing the signal to the bridge data signal. The Gaussian envelope has been created by the function 8.2. The 1.7 in front multiplies the signal to to achieve the desired amplitude. The .4 in the power results in the desired width of the envelope. The 2.8 shifts the envelope over the time axis.

$$1.7e^{(\frac{t-2.8}{.4})^2} \tag{8.2}$$

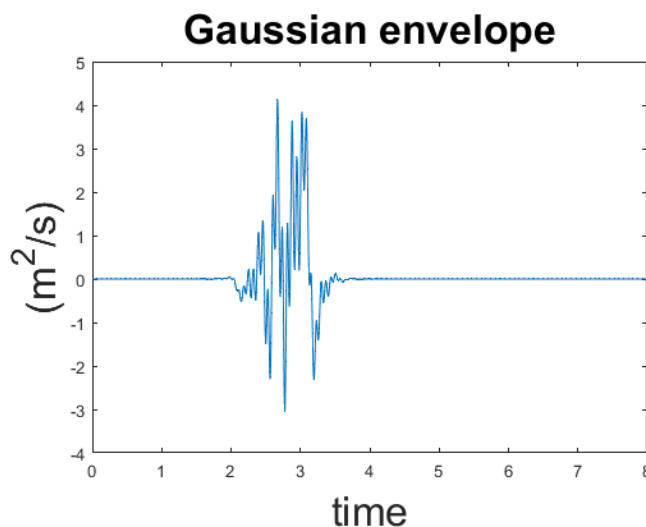


Figure 8.8: Gaussian envelope combined with 5 sinusoidal signals

### 8.5.2. Bridge signal

For testing the mechanism under bridge excitations, a section of 65 seconds has been selected from the dataset. This section is displayed in Figure 8.9.

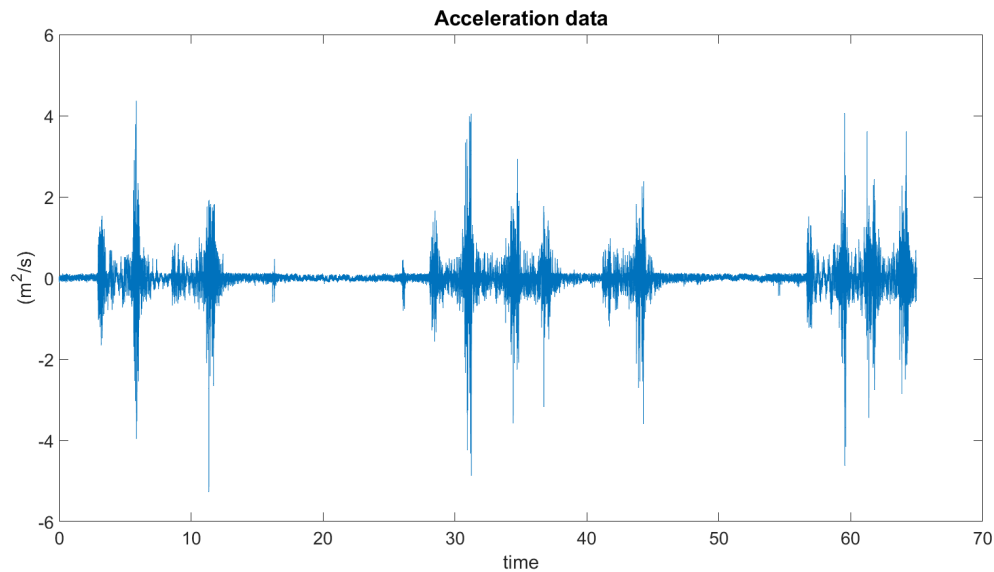


Figure 8.9: Input accelerations from bridge dataset for shaker test.

### 8.5.3. Stored energy from bridge specific excitations

The mechanism is not able to harvest energy under the bridge specific excitations. The combination of amplitude and acceleration are too low to achieve rotation of the proof mass in the current set-up.

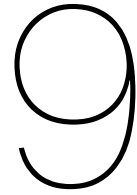
Despite the inability of the mechanism was not being able to harvest energy from the bridge vibrations during the tests, the conclusion that this type of mechanism is not suitable for harvesting such vibrations can not be drawn. With alteration of the system parameters, rotation of the mass under these low amplitude, low acceleration vibrations could be achieved. One of these alterations is reducing the rotational inertia. This lower inertia would reduce the resistance of the mass to start rotating, and might allow the mechanism to work in lower energy environments such as the bridge vibrations. As a result there would also be less energy stored at the same rotational speed which would likely mean that the harvesting moment of the spring needs to be reduced. While this could increase performance in lower energy environments, at higher energy environment performance could decrease.

## 8.6. Test results

Combining all test results, it can be concluded that the mechanism is able to harvest energy from harmonic vibrations as well as shocks under certain conditions. The ability of harvesting energy from the vibration depends on the amplitude and acceleration of the vibrations. With a higher acceleration, energy from smaller amplitude vibrations can be harvested.

The vibrations from the bridge measurements do not meet these conditions for the current system parameters, as the mechanism is not able to harvest energy during simulated bridge vibrations. As mentioned, depending on the vibrations, altering the rotational inertia can increase the performance of the harvester. The mechanism can additionally be improved, especially for lower energy environments, by further reducing the engagement angle.

Apart from the test, during handling of the harvester, it is observed that the mechanism is also able to harvest energy from orientation changes. This is not quantified with tests.



# Conclusion and Discussion

## 9.1. Discussion

As this research has focused on the take-off of part of the energy harvester, there are no results on actual stored energy of the harvester. This makes comparison with other harvesters challenging for the standardised tests, as the performance of the harvester is usually evaluated by comparing stored electrical energy.

The production of the harvester is rather rudimentary and can improve a lot, so results from this proof of concept would not display the full potential of the design. Especially the ratchet mechanism allows for improvement. No research on or commercially available ratchet systems were found that allow for translation of a rotational center of a mass. Next to the building quality, the model is also quite rudimentary. In hindsight, choosing to focus on a smaller region of the research might have given less, but better results.

## 9.2. Conclusion

The goal of the research was to design a new type of energy harvester for application on bridges and build a proof-of-concept. Comparing the design to literature, the design is new in the sense that no inertial take-off mechanisms have been found with a translating and rotating proof mass. To evaluate the performance of the harvester, it has been tested under specific and general excitations. Under harmonic excitation, the mechanism is able to harvest energy from a wide range of frequencies (10 – 20Hz) and at low accelerations (4g) as well as shocks at .4g.

The designed harvester is, as intended, able to harvest energy from various types of ground excitations at low frequency under intermittent conditions. The conditions on that have been measured on the bridge, however, do not fall into the range where the mechanism is able to harvest with the current system parameters.

Answering the research question, newly designed harvester is, with the system parameters from the proof of concept not able outperform current energy harvesters, because the mechanism does not store energy when subjected to simulated bridge excitations.

### 9.2.1. Prototype

A next step would be the production of a prototype with parts especially developed for the design. All parts of the mechanism can be improved. The ratchet should be produced with higher tolerances and a smaller engagement angle. Instead of the spring and carriage system that was used in the proof of concept, the chosen system of parallel flexures should be designed and produced. A constant torque spring will need to be developed that is up to desired specifications on the harvesting moment. For the low energy ground vibrations, changes in the system parameters have been proposed that could lead to improved performance. The proposed system parameters for are a decrease in rotational inertia relative to the linear inertia and a (further) decrease in engagement angle.

### **9.2.2. Model**

System parameters from the produced prototype should be measured. With information of these tests, sensors in place that measure rotation and translation. This improved data acquisition will give more insight in the dynamic behaviour of the harvester over time, where as the current method only takes into account the amount of stored energy. With improved data acquisition, and thus data of the mechanism over time, the performance of the model can be reviewed and increased, while also evaluate the impact of simplifications.

### **9.2.3. Transduction**

In the proof of concept, transduction does not take place. For the prototype, an system needs to be developed, that disengages with the rotation of the proof mass and engages with a transducer. An appropriate transducer will need to be chosen or developed.

### **9.2.4. Alternative application**

Next to the proposed alterations that can be made such that the system parameters might be able to harvest energy from bridge vibrations, the mechanism could be applied in other applications where ambient vibrations are intermittent or of varying frequency. Depending on the application, dimensions of the mechanism can be altered to suit the demands, but in with the current system parameters, this would need to be an environment where higher accelerations are found than in the bridge environment.

# Bibliography

- Bibo, A., Masana, R., King, A., Li, G., & Daqaq, M. (2012). Electromagnetic ferrofluid-based energy harvester. *Physics Letters A*, 376(32), 2163–2166. <https://doi.org/https://doi.org/10.1016/j.physleta.2012.05.033>
- Blad, T. (2021). Micro energy harvesting from low-frequency vibrations : Towards powering pacemakers with heartbeats. *DANS*. <https://doi.org/https://doi.org/10.4233/uuid:eeebed12-090f-4a4b-8450-d05a763fc9da>
- Blad, T. W., & Tolou, N. (2019). On the efficiency of energy harvesters: A classification of dynamics in miniaturized generators under low-frequency excitation. *Journal of Intelligent Material Systems and Structures*, 30(16), 2436–2446. <https://doi.org/10.1177/1045389X19862621>
- Bonisoli, E., Repetto, M., Manca, N., & Gasparini, A. (2017). Electromechanical and electronic integrated harvester for shoes application. *IEEE/ASME Transactions on Mechatronics*, 22(5), 1921–1932. <https://doi.org/10.1109/TMECH.2017.2667401>
- Covaci, C., & Gontean, A. (2020). Piezoelectric energy harvesting solutions: A review. *Sensors*, 20(12). <https://doi.org/10.3390/s20123512>
- Fan, K., Zhang, Y., Liu, H., Cai, M., & Tan, Q. (2019). A nonlinear two-degree-of-freedom electromagnetic energy harvester for ultra-low frequency vibrations and human body motions. *Renewable Energy*, 138, 292–302. <https://doi.org/https://doi.org/10.1016/j.renene.2019.01.105>
- FrictionPhysics. (n.d.). *One-way clutch history and metal fatigue*. <https://frictionphysics.com/history.html>
- Fu, H., Mei, X., Yurchenko, D., Zhou, S., Theodossiades, S., Nakano, K., & Yeatman, E. M. (2021). Rotational energy harvesting for self-powered sensing. *Joule*, 5(5), 1074–1118. <https://doi.org/https://doi.org/10.1016/j.joule.2021.03.006>
- Galchev, T. V., McCullagh, J., Peterson, R. L., & Najafi, K. (2011). Harvesting traffic-induced vibrations for structural health monitoring of bridges. *Journal of Micromechanics and Microengineering*, 21(10), 104005. <https://doi.org/10.1088/0960-1317/21/10/104005>
- Gutierrez, M., Shahidi, A., Berdy, D., & Peroulis, D. (2015). Design and characterization of a low frequency 2-dimensional magnetic levitation kinetic energy harvester. *Sensors and Actuators A: Physical*, 236, 1–10. <https://doi.org/https://doi.org/10.1016/j.sna.2015.10.009>
- Hadas, Z., Vetiska, V., Singule, V., Andrs, O., Kovar, J., & Vetiska, J. (2012). Energy harvesting from mechanical shocks using a sensitive vibration energy harvester. *International Journal of Advanced Robotic Systems*, 9(5), 225. <https://doi.org/10.5772/53948>
- Halim, M. A., Cho, H., & Park, J. Y. (2015). Design and experiment of a human-limb driven, frequency up-converted electromagnetic energy harvester. *Energy Conversion and Management*, 106, 393–404. <https://doi.org/https://doi.org/10.1016/j.enconman.2015.09.065>
- He, M., Wang, S., Zhong, X., & Guan, M. (2019). Study of a piezoelectric energy harvesting floor structure with force amplification mechanism. *Energies*, 12(18). <https://doi.org/10.3390/en12183516>
- Ibrahim, A., Ramini, A., & Towfighian, S. (2020). Triboelectric energy harvester with large bandwidth under harmonic and random excitations. *Energy Reports*, 6, 2490–2502. <https://doi.org/https://doi.org/10.1016/j.egyr.2020.09.007>
- Ibrahim, S. W., & Ali, W. G. (2012). A review on frequency tuning methods for piezoelectric energy harvesting systems. *Journal of Renewable and Sustainable Energy*, 4(6), 062703. <https://doi.org/10.1063/1.4766892>
- Jackson, N., Stam, F., Olszewski, O. Z., Houlihan, R., & Mathewson, A. (2015). Broadening the bandwidth of piezoelectric energy harvesters using liquid filled mass [Eurosensors 2015]. *Procedia Engineering*, 120, 328–332. <https://doi.org/https://doi.org/10.1016/j.proeng.2015.08.627>
- Jiang, J., Liu, S., Feng, L., & Zhao, D. (2021). A review of piezoelectric vibration energy harvesting with magnetic coupling based on different structural characteristics. *Micromachines*, 12(4). <https://doi.org/10.3390/mi12040436>

- Jiang, W., Wang, L., Zhao, L., Luo, G., Yang, P., Ning, S., Lu, D., & Lin, Q. (2021). Modeling and design of v-shaped piezoelectric vibration energy harvester with stopper for low-frequency broadband and shock excitation. *Sensors and Actuators A: Physical*, *317*, 112458. <https://doi.org/https://doi.org/10.1016/j.sna.2020.112458>
- Ju, S., & Ji, C.-H. (2018). Impact-based piezoelectric vibration energy harvester. *Applied Energy*, *214*, 139–151. <https://doi.org/https://doi.org/10.1016/j.apenergy.2018.01.076>
- Kuehnert, J., Mangeney, A., Capdeville, Y., Metaxian, J.-P., Bonilla, L., Stutzmann, E., Chaljub, E., Boissier, P., Brunet, C., Kowalski, P., Lauret, F., & Hibert, C. (2020). Simulation of topography effects on rockfall-generated seismic signals: Application to piton de la fournaise volcano.
- Ledecz, Á., Hay, T., Volgyesi, P., Hay, D. R., Nadas, A., & Jayaraman, S. (2009). Wireless acoustic emission sensor network for structural monitoring. *IEEE Sensors Journal*, *9*(11), 1370–1377. <https://doi.org/10.1109/JSEN.2009.2019315>
- Luo, A., Zhang, Y., Dai, X., Wang, Y., Xu, W., Lu, Y., Wang, M., Fan, K., & Wang, F. (2020). An inertial rotary energy harvester for vibrations at ultra-low frequency with high energy conversion efficiency. *Applied Energy*, *279*, 115762. <https://doi.org/https://doi.org/10.1016/j.apenergy.2020.115762>
- Maamer, B., Boughamoura, A., Fath El-Bab, A. M., Francis, L. A., & Tounsi, F. (2019). A review on design improvements and techniques for mechanical energy harvesting using piezoelectric and electromagnetic schemes. *Energy Conversion and Management*, *199*, 111973. <https://doi.org/https://doi.org/10.1016/j.enconman.2019.111973>
- Mosey, S., Charlton, P., & Wells, I. (2013). Resolution enhancement of ultrasonic b-mode images. *Insight - Non-Destructive Testing and Condition Monitoring*, *55*. <https://doi.org/10.1784/insi.2012.55.2.78>
- Phillips, C. L., & Harbor, R. D. (1996). *Feedback control systems / charles l. phillips, royce d. harbor.* (3rd ed.). Prentice Hall.
- Pillatsch, P., Yeatman, E. M., & Holmes, A. S. (2012). A scalable piezoelectric impulse-excited energy harvester for human body excitation. *Smart Materials and Structures*, *21*(11), 115018. <https://doi.org/10.1088/0964-1726/21/11/115018>
- Salem, M. S., Ahmed, S., Shaker, A., Alshammari, M. T., Al-Dhlan, K. A., Alanazi, A., Saeed, A., & Abouelatta, M. (2021). Bandwidth broadening of piezoelectric energy harvesters using arrays of a proposed piezoelectric cantilever structure. *Micromachines*, *12*(8). <https://doi.org/10.3390/mi12080973>
- Sari, I., Balkan, T., & Kulah, H. (2008). An electromagnetic micro power generator for wideband environmental vibrations [Special Issue: Transducers/07 Eurosensors XXI, The 14th International Conference on Solid State Sensors, Actuators and Microsystems and the 21st European Conference on Solid-State Transducers]. *Sensors and Actuators A: Physical*, *145-146*, 405–413. <https://doi.org/https://doi.org/10.1016/j.sna.2007.11.021>
- Sarwar, M. Z., & Park, J.-W. (2020). Bridge displacement estimation using a co-located acceleration and strain. *Sensors*, *20*(4). <https://doi.org/10.3390/s20041109>
- Shi, G., Chen, J., Peng, Y., Shi, M., Xia, H., Wang, X., Ye, Y., & Xia, Y. (2020). A piezo-electromagnetic coupling multi-directional vibration energy harvester based on frequency up-conversion technique. *Micromachines*, *11*(1). <https://doi.org/10.3390/mi11010080>
- Talib, N. H. H. A., Salleh, H., Youn, B. D., & Resali, M. S. M. (2019). Comprehensive review on effective strategies and key factors for high performance piezoelectric energy harvester at low frequency. *International Journal of Automotive and Mechanical Engineering*, *16*(4), 7181–7210. <https://doi.org/10.15282/ijame.16.4.2019.03.0537>
- Tang, L., & Yang, Y. (2012). A nonlinear piezoelectric energy harvester with magnetic oscillator. *Applied Physics Letters*, *101*(9), 094102. <https://doi.org/10.1063/1.4748794>
- Wang, L., Todaria, P., Pandey, A., O'Connor, J., Chernow, B., & Zuo, L. (2016). An electromagnetic speed bump energy harvester and its interactions with vehicles. *IEEE/ASME Transactions on Mechatronics*, *21*(4), 1985–1994. <https://doi.org/10.1109/TMECH.2016.2546179>
- Xie, L., & Du, R. (2012). Harvest human kinetic energy to power portable electronics. *Journal of Mechanical Science and Technology*, *26*, 2005–2008.
- Xue, T., Yeo, H. G., Trolier-McKinstry, S., & Roundy, S. (2018). Wearable inertial energy harvester with sputtered bimorph lead zirconate titanate (PZT) thin-film beams. *Smart Materials and Structures*, *27*(8), 085026. <https://doi.org/10.1088/1361-665x/aad037>

- Yang, Y., Pian, Y., & Liu, Q. (2019). Design of energy harvester using rotating motion rectifier and its application on bicycle. *Energy*, *179*, 222–231. <https://doi.org/https://doi.org/10.1016/j.energy.2019.05.036>
- Yeatman, E. M. (2008). Energy harvesting from motion using rotating and gyroscopic proof masses. *Proceedings of the Institution of Mechanical Engineers, Part C: Journal of Mechanical Engineering Science*, *222*(1), 27–36. <https://doi.org/10.1243/09544062JMES701>
- Ylli, K., Hoffmann, D., Willmann, A., Becker, P., Folkmer, B., & Manoli, Y. (2015). Energy harvesting from human motion: Exploiting swing and shock excitations. *Smart Materials and Structures*, *24*(2), 025029. <https://doi.org/10.1088/0964-1726/24/2/025029>
- Zhang, Y., Wang, T., Luo, A., Hu, Y., Li, X., & Wang, F. (2018). Micro electrostatic energy harvester with both broad bandwidth and high normalized power density. *Applied Energy*, *212*, 362–371. <https://doi.org/https://doi.org/10.1016/j.apenergy.2017.12.053>
- Zou, H.-X., Zhang, W.-M., Wei, K.-X., Li, W.-B., Peng, Z.-K., & Meng, G. (2016). A Compressive-Mode Wideband Vibration Energy Harvester Using a Combination of Bistable and Flextensional Mechanisms [121005]. *Journal of Applied Mechanics*, *83*(12). <https://doi.org/10.1115/1.4034563>